

F-POS-K1 AN IMPROVED MODEL OF POINT MUTATIONS IN PROTEIN SEQUENCES. R.M. Schwartz and M.O. Dayhoff. National Biomedical Research Foundation, Georgetown University Medical Center, 3900 Reservoir Road, N.W., Washington, D.C. 20007

A representation of the point mutation process based on amino acid mutabilities and their replacement probabilities is essential for understanding protein evolution. In particular, the detection of distant relationships between proteins must rely on a method of scoring residue by residue comparisons. We have constructed a new, improved scoring matrix for these purposes on the basis of currently available sequence data. This includes 1570 amino acid substitutions in over 60 groups of sequences less than 15 percent different. We had previously constructed such a matrix on the basis of 779 amino acid substitutions in 11 groups of sequences about 20 percent different. The new matrix has obvious differences from our earlier matrix: the nondiagonal elements are less extreme and the substitutions involving highly conserved residues appear to reflect the genetic code more closely. In preliminary tests using both our segment comparison and alignment score programs, this new matrix scores known relationships higher thus producing a better separation between related and unrelated sequences. We will display comparisons of our new matrix with other scoring matrices, using both real and simulated sequences.

Supported by NIH grants GM 08710 and NASA grant NASW 2848.

F-POS-K2 SCREENING PROTEIN SEQUENCES FOR EVIDENCE OF GENE DUPLICATION. W.C. Barker, L.K. Ketcham*, and M.O. Dayhoff. National Biomedical Research Foundation, Georgetown University Medical Center, 3900 Reservoir Road, N.W., Washington, D.C. 20007

We examined sequences from all of the 116 superfamilies of sequenced proteins for evidence of internal duplication using the computer program RELATE, the mutation data scoring matrix, and a segment length of 20 for proteins > 50 residues long, and 12 for proteins < 50 residues long. Proteins from 16 superfamilies scored at least 3.0 SD above the average for randomized sequences with the same composition. Three types of intragenic duplications were detected: (1) One or more duplications of nearly an entire gene, producing a protein for which two to four detectable regions of sequence homology constitute nearly the entire sequence (of five such types of proteins, two have evidence of an even more ancient duplication to form the prominent homology region); (2) Reduplication of a small gene segment to produce a protein that is repetitive over most of its length (three examples were detected); and (3) Partial duplication within a gene to produce a protein with regions of sequence similarity not involving the entire chain (eight examples fell into this category). We believe that all of these proteins yielding high scores reflect real duplications. We also investigated the limits of detection of ancient duplications using sequences derived by random mutation of a model sequence consisting of ten 10-residue repeats. The original repetitive nature of the sequence was usually detected after 250 point mutations even though the ancestral segment could not be accurately reconstructed or detected by eye. Supported by NIH grants HD 09547, GM 08710, and RR 05681.

F-POS-K3 SCREENING PROTEIN SEQUENCES FOR EVIDENCE OF RELATIONSHIP. B.C. Orcutt* and M.O. Dayhoff, National Biomedical Research Foundation, Georgetown University Medical Center, 3900 Reservoir Road, N.W., Washington, D.C. 20007

Protein sequences of detectable evolutionary relationship typically have a wide phylogenetic distribution, usually in a whole group such as the vertebrates and often in all eukaryotes or all living things. For each new type of protein sequence reported, we perform a primary screening, using the computer program SEARCH, to detect any related sequences. The optimization of the screening procedure is considered here. Typically a segment of 25 residues of the new sequence is compared with all 25-residue segments and the shorter end segments of each known sequence. An input matrix of amino acid pair scores is supplied to the program. For the best matrix, based on mutation data, all related sequences less than 60% different typically appear above the distribution of scores of unrelated sequences, while more distantly related sequences appear in the upper tail. Quantitative results will be displayed comparing a number of variations on the mutation data matrix and the search procedures. The 1976 mutation data matrix, containing twice as much data as the 1969 version, is clearly superior to it and both are far superior to either the genetic code or unitary matrices.

Supported by NIH grants GM 08710 and RR 05681.

F-POS-K4 BROWNIAN MOTION OF THE ENDS OF FLEXIBLE OLIGOMER MOLECULES RELATIVE TO ONE ANOTHER AS ESTIMATED BY ENERGY TRANSFER BETWEEN THE CHAINS ENDS. E. Haas*, E. Katchalski-Katzir, and I.Z. Steinberg*, The Weizmann Institute of Science, Rehovot, Israel.

A series of homologous oligopeptides containing a donor and an acceptor of excitation energy at their ends was prepared. The chromophore-bearing oligopeptides studied are: Dansyl-(N^5 -(2-hydroxyethyl)-L-glutamyl)- n -DL- β -naphthylalanine, ($n=4-9$). The kinetics of fluorescence decay of the donor (β -methyl-naphthyl moiety) were measured in glycerol/TFE (trifluoroethanol) mixtures of various viscosities. None of the experimentally obtained fluorescence decay curves could be adequately described by simple monoexponential function. Based on the best estimates it was shown qualitatively that average lifetimes decrease markedly on increasing the relative content of TFE in the glycerol/TFE solvent mixture, i.e. on decreasing the viscosity of the medium. The lifetime of the donor in an oligopeptide lacking an acceptor is monoexponential and varied by less than 5% in the above solvent mixtures. We ascribe these results to the increase in the efficiency of energy transfer, as a result of an increase in the rate of intramolecular Brownian motion of the donor and acceptor, evoked by a corresponding decrease in medium viscosity. Using a modified Fick equation and a curve fitting procedure the intramolecular diffusion coefficients for the chain ends, D , were obtained from the donor fluorescence decay curves, $I(t)$. Values of $0.05 - 1 \times 10^{-7} \text{ cm}^2 \text{ sec}^{-1}$ for D were obtained with the viscosity of solution varying from 1 to 200 cp. This value is by about an order of magnitude lower than that of the diffusion coefficients expected for small molecules. This shows that for all of the oligopeptides studied the internal friction is finite and appreciable. Furthermore, the internal friction is higher for the shorter chain molecules. It thus follows that the shorter chains cannot permit as much flexibility of motion to their ends as the longer chains do.

F-POS-K5 ENTHALPIES FOR SUBUNIT ASSOCIATION AT SUCCESSIVE STAGES OF OXYGEN BINDING IN HUMAN HEMOGLOBIN. Frederick C. Mills* and Gary K. Ackers, Department of Biochemistry, University of Virginia, Charlottesville, Virginia 22901.

Oxygenation curves of human hemoglobin have been measured as a function of protein concentration at several different temperatures in order to determine Van't Hoff enthalpies of oxygenation-linked dimer-tetramer association. We find that the -32 kcal difference between heats of subunit association in unliganded and fully oxygenated states is partitioned as follows: for deoxy and singly-liganded tetramer the heats of assembly differ by -10 kcal; a -22 kcal difference is found between the heats of assembly for singly and triply-liganded tetramer; there is essentially no difference between the heats of assembly for triply-liganded and fully-liganded tetramers. Under the same conditions (0.1 M Tris HCl, 0.1 M NaCl, 1 mM Na₂EDTA, pH 7.4) we find values of -14.9 kcal/mole for oxygenating isolated α chains and -16.9 kcal/mole for isolated β chain oxygenation. Over the temperature range 10°-33° the concentration-dependent oxygenation curves reflect essentially noncooperative dimers and no difference between the free energies of association for triply and fully liganded tetramers. The overall enthalpy for binding two moles of oxygen to a mole of dissociated dimers is -32 kcal, while the values for isolated chains sum to -31.8 kcal/2 moles O₂. The enthalpy for fully oxygenating tetramers under these conditions can be resolved into successive binding steps as follows: -6 kcal/mole O₂ for the first oxygen; -10 kcal/2 moles O₂ for the middle two steps, and -16 kcal/mole O₂ for the last step. Thus the release of constraints within tetrameric hemoglobin with successive oxygen binding steps is accompanied by increasing negative stepwise binding enthalpies as well as free energies, and all constraints are released by the third binding step. Supported by grants from NSF and NIH.

F-POS-K6 MAGNETIC RESONANCE STUDY OF THE INTERACTION OF Mn^{2+} WITH HUMAN HEMOGLOBIN.

Raj K. Gupta and Jeffrey L. Benovic*, Institute for Cancer Research, Philadelphia, Pa. 19111

Magnetic resonance measurements reveal that Mn^{2+} , a paramagnetic probe, interacts with hemoglobin in 0.02 M bis-Tris buffer, pH 7.2 and 0.15 M NaCl at 23°C. Addition of oxyhemoglobin free of 2,3 DPG to a solution containing Mn^{2+} results in a decrease in the observed EPR signal reflecting binding of Mn^{2+} to the protein. A Scatchard plot of free Mn^{2+} at several levels of total Mn^{2+} and hemoglobin yielded four Mn^{2+} binding sites per tetramer with a dissociation constant (K_D^{Mn}) of $\sim 5 \text{ mM}$. The binding of Mn^{2+} to oxyhemoglobin also enhances the paramagnetic effect of Mn^{2+} on the relaxation rate ($1/T_1$) of water protons. An analysis of the titration curves measuring $1/T_1$ of water protons at several levels of Mn^{2+} and oxyhemoglobin yielded a bound state enhancement (ϵ_b) of 9.5 and a value of K_D^{Mn} in agreement with the EPR data. Addition of Zn^{2+} to a solution containing Mn^{2+} and oxyhemoglobin de-enhances the $1/T_1$ of water protons due to a partial displacement of hemoglobin bound Mn^{2+} by Zn^{2+} yielding a K_D^{Zn} of $\sim 1.5 \text{ mM}$. Deoxygenation or the presence of 0.1 M Mg^{2+} have no appreciable effect on the amount of free Mn^{2+} or on the enhancement of $1/T_1$ of water protons by Mn^{2+} . At the physiological levels of Mg^{2+} and Zn^{2+} in red cells, only a very small fraction of the total hemoglobin present could be complexed to these cations at the sites detected here, arguing against any physiological role of these Mn^{2+} binding sites in regulating oxygen affinity. (Supported in part by USPHS RCDA AM-00231 and USPHS grant AM-19454).

F-POS-K7 PROTON NUCLEAR MAGNETIC RESONANCE STUDIES OF THE OXYGENATION OF HUMAN ADULT HEMOGLOBIN. G. Viggiano and C. Ho, Department of Life Sciences, University of Pittsburgh, Pittsburgh, Pa. 15260

Proton nuclear magnetic resonance (NMR) at 250 MHz using the correlation spectroscopy mode has been employed to investigate the binding of oxygen to human adult hemoglobin (Hb A) in D₂O medium at pD 7. The hyperfine shifted proton resonances of deoxy Hb A over the spectral region -7 to -20 ppm, downfield from the proton resonance of residual water in the sample, provide a direct way to measure the binding of oxygen to α and β chains of Hb A. A systematic study of the effects of organic phosphates, such as 2,3-diphosphoglycerate (DPG) and inositol hexaphosphate (IHP), on the cooperative oxygenation of Hb A has been carried out. Our present results have confirmed our early work [Johnson and Ho, *Biochemistry* **13** 3653 (1974)], namely the α chains of Hb A have a higher affinity for oxygen as compared to those of the β chains in the presence of organic phosphates. In addition, an analysis of the resonance intensity and line shape of the β -heme resonance at -18 ppm from HDO provides a means to monitor the structural changes of the hemoglobin molecule upon oxygenation. The relationship of our results to the mechanism of cooperative oxygenation of hemoglobin will be discussed. (This work is supported by research grants from NIH.)

F-POS-K8 STRUCTURAL AND FUNCTIONAL STUDIES ON HEMOGLOBINS WITH MODIFIED HEME GROUPS.

David W. Seybert^{*}, James F. Deatherage^{*}, and Keith Moffat, Section of Biochemistry, Molecular & Cell Biology, Cornell University, Ithaca, New York 14853.

A series of horse hemoglobin derivatives was prepared, containing modified heme groups of two different types. In the first, the 2- and 4-substituents of the hemes, which are vinyl groups in naturally occurring protoheme, were replaced by hydrogen, methyl, ethyl, bromine or formyl groups; in the second, the sixth ligand of the iron, which is water in methemoglobin, was replaced by cyanide, azide, fluoride, or nitric oxide. Equilibrium and kinetic studies of ligand binding were carried out on all the first type, and the structures of two of them (with hydrogen and ethyl substituents) were determined by X-ray difference Fourier crystallographic techniques. Surprisingly, complete removal of the vinyl groups had a much smaller effect on both the structural and the functional properties than their reduction to ethyl groups. Ligand association rates were insensitive to the electronic nature of the 2- and 4-substituents, but the dissociation rates were directly dependent on their electron-withdrawing properties. The structures of all the derivatives of the second type were also determined crystallographically. The conformation of the ligand pocket is clearly extremely sensitive to the nature of the ligand; all liganded hemoglobins differ in structure. We conclude that a rate-determining step in the ligand dissociation reaction is rupture of the iron - ligand bond, and that this is controlled by the electronic properties of the heme. In contrast, a rate-determining step in the ligand association reaction is a slight opening of the ligand pocket; this is necessary for those ligands such as cyanide and carbon monoxide which bind in a linear, end-on mode to the iron, but not for oxygen and nitric oxide which bind in a bent, end-on mode.

F-POS-K9 REACTION OF THE MASKED SULFHYDRYLS OF HEMOGLOBIN WITH MERCURIC CHLORIDE; EFFECTS ON ALKALINE DENATURATION. A.H. Burr, E.M. Reimer^{*}, and G. Watson^{*}, Dept. of Biological Sciences, Simon Fraser Univ., Burnaby, British Columbia, Canada V5A 1S6 and Robley C. Williams, Jr., Dept. of Molecular Biology, Vanderbilt Univ., Nashville 37235.

The concentration of HgCl₂ was followed amperometrically with a rotating platinum electrode whose potential with respect to a standard calomel electrode was maintained by a feedback amplifier. The reaction with the 6 SH's of liganded human hemoglobin occurred at different rates. That with the two 893 cysteine SH's was faster than the \sim 3 sec mixing time. That with each of the masked SH pairs was slower and was approx. 2nd order as demonstrated by curve fitting. The more reactive of the masked pairs was identified by first reacting oxyhemoglobin with 1 to 6 equivalents of HgCl₂ then heat denaturing the tetramers, separating the α - and β - subunits by disc acrylamide gel electrophoresis and determining the Hg content of each subunit by X-ray fluorescence spectroscopy. The first 4 equivalents reacted primarily with the 4 SH's on the β subunits, and the last two primarily with the α 104 SH's. Thus the decreasing order of reactivity is: 893, β 112, α 104.

Perutz (1974) proposed that ionization of the masked SH's, located in the α ₁ β ₁ interface, is chiefly responsible for the sensitivity of HbA to alkaline denaturation. The effect of blocking the ionization of each SH type with HgCl₂ indicates more than one factor, however. The denaturation data was fit as 2 parallel 1st order reactions. The fraction of the more slowly denaturing form of HbA increases from 20% to 80% as the β 112 SH's are blocked, but is insensitive to blocking of the 893 or α 104 SH's. On the other hand, the rate constant for the slower reaction is decreased by blocking primarily the 893 SH's, and that for the faster reaction is decreased by blocking any of the 3 SH types.

F-POS-K10 CHARACTERIZATION OF FLUORESCCEIN CONJUGATES OF CYTOCHROME C. J.A. Thomas and P.C. Hsu*, Biochemistry Section, Division of Biochemistry, Physiology and Pharmacology, The University of South Dakota School of Medicine, Vermillion, South Dakota 57069

Fluorescein isothiocyanate reacts with the epsilon amino groups of lysyl residues in cytochrome c at pH 8. Four of the nineteen possible derivatives predominate, and have been isolated by ion exchange chromatography. Each derivative has one fluorescein per molecule of cytochrome c, based on a molar extinction coefficient of 74,000 at 494 nm for fluorescein conjugates. The ascorbate-reduced minus oxidized difference spectrum for each derivative is identical with native cytochrome c, as is the 695 nm absorption band, indicating the fluorescein does not alter the heme spectrum. However, the fluorescein absorption band varies slightly with each derivative, suggesting different microenvironments of this chromophore. As compared to native cytochrome c, each derivative has different kinetic constants in the succinate-cytochrome c reductase and cytochrome oxidase assays. Derivatives I, II and IV no longer have a high affinity site for cytochrome oxidase, while derivative III has a normal K_m but a V_{max} only 23% of normal. In the reductase assay, derivative II has a K_m twice normal, but a V_{max} only 3% of normal. The other derivatives have all lost their high affinity site. The K_m and V_{max} values for the low affinity sites vary independently from the behavior of the high affinity sites. The data are consistent with the existence of four kinds of reaction sites on cytochrome c, with separate high and low affinity sites for both the oxidase and reductase. [Supported by grant 75-DA-605 from the American Heart Association, Dakota Affiliate, and grant GM 22845 from NIH.]

F-POS-K11 PREPARATION AND PRELIMINARY CHARACTERIZATION OF A BIOLOGICALLY ACTIVE FLUORESCENT CONJUGATE OF INSULIN. C. Karp, V. Glushko, M. Sonenberg and H. M. Katzen*, Sloan-Kettering Institute for Cancer Research, New York, N.Y., 10021, and Merck Institute for Therapeutic Research, Rahway, N.J., 07065.

Several current models of peptide hormone action stress the role of the transduction mechanism by which extracellular components can regulate intracellular processes without entering the cell. The kinetics of specific binding of ^{125}I insulin to cell surface receptors, as described by a number of laboratories, do not reflect a simple relationship, with evidence of negative cooperativity and multiple sites. In order to follow dynamic changes in the insulin-receptor environment, dansyl conjugates of insulin were prepared. Based on the distribution probability for a single modification as a function of pH, the dansylation conditions were chosen to preferentially label tyrosine. The insulin monomer, found to contain an average of 1.2 dansyls per molecule, was separated from the free dye and non-dissociable insulin dimer by gel filtration. Two-dimensional TLC and amino acid analysis demonstrated that modification occurred primarily (>80%) at tyrosine, although glycine and phenylalanine derivatives were detected. Further purification was accomplished by ion exchange and phase partition chromatography; however, the most useful procedure was preparative isoelectric focusing on Sephadex G-75 in 7M urea, which produced one major (dansyl-tyrosine) and four minor fluorescent insulin bands. Although the non-dissociable dimer and N-terminal derivatives were found to be inactive, the tyrosine labeled conjugates appeared one-third as effective as unmodified insulin in stimulating glucose conversion into CO_2 by isolated fat cells. Furthermore, upon incubation with anti-insulin sera, the quantum yield showed a 3.2 fold increase, which could be blocked by $10^{-4}M$ native insulin. (Supported in part by grants from the NCI, CA-08748 and CA-16889, and from NIH, AM-18759).

F-POS-K12 CONFORMATION OF MYELIN BASIC PROTEIN AND ENCEPHALITOGENIC PEPTIDE BY NMR. W.J. Moore, B.E. Chapman*, L. Littlemore*, and S.J. Pasariibu*, School of Chemistry, University of Sydney, N.S.W. 2006, Australia.

High resolution ^{13}C and 1H NMR spectra of myelin basic protein over a range of pH and concentrations indicate an intramolecular folding of the polypeptide chain occurs in aqueous solution in the region of residues 85 to 116. As the pH is raised and the positive charge on the protein reduced from 28 to 18, intermolecular aggregation occurs, which appears to involve these same folded regions. The only arginine residue methylated by endogenous brain enzyme is at 107. Methylation with ^{13}C enriched S-adenosylmethionine introduces a specific marker at 107 that can be used as a probe of the environment in that region. The encephalitogenic determinant in guinea pig from residues 114 to 122 has been synthesized and individual carbon resonances are compared in the nonapeptide and the protein. The region of the protein involved in folding and substrate specificities is conservative in various species and we can surmise that it may have a specialized role in protein-lipid interactions in the myelin membrane.

F-POS-K13 EQUALITY IN THE NUMBER OF TRITON X-114 MOLECULES BINDING TO DIFFERENT SERUM ALBUMINS. Wayne W. Sukow, Department of Physics, University of Wisconsin-River Falls, River Falls, WI 54022.

Serum albumin is a ubiquitous transport protein which occurs far back on the evolutionary scale. Evolutionary changes, especially within a species, seem to be conservative with respect to amino acid composition and molecular weight. A study of the binding of TRITON X-114, at the maximum free monomer concentration of this nonionic detergent, to different mammalian serum albumins shows there is only a small variation within a species in the number of TRITON X-114 molecules bound. Binding to rat, guinea pig, rabbit, canine, goat, sheep, human, porcine, bovine and chicken serum albumin in pH 7.0 phosphate buffer at 16°C was studied. The average number bound (ν) ranges from 4.0 ± 1 for canine to 6.3 ± 1 for porcine serum albumin. A value of $\nu = 3.8 \pm 3$ for chicken serum albumin suggests there is little variation between species. Translating the number of TRITON X-114 molecules bound into the number of binding sites for these molecules on serum albumins suggests an equality in the number of binding sites. This equality in number of sites would support the view that the tertiary structure of these serum albumins is similar. The values of ν are small enough that a detailed study of the binding will be possible enabling one to determine a unique binding model for these systems.

Supported by University of Wisconsin-River Falls Research Grant 0795-2-75.

F-POS-K14 HIGH ORDERS OF REACTION IN THE PHASE TRANSFER OF PROTEINS BY LIGAND BINDING. R. V. Mustacich and Gregorio Weber, Department of Biochemistry, University of Illinois, Urbana, Illinois 61801

The on and off switching of chemical functions in the course of metabolic regulation presupposes sensing the concentration of a metabolite, accomplished by its specific binding to protein. The chemical switching is the more effective the narrower the range of ligand concentration over which the change takes place. The effectiveness is measured by the Hill coefficient H which gives the change in the logarithm of the ratio of bound to unbound sensing sites per logarithmic unit change in ligand concentration. If a protein with N binding sites is transferred between two phases following addition, by a reaction of order J , of a ligand with partition free energy between the phases δF_1^0 , and if each ligand protein complex is stabilized in the upper phase by the same free energy δF_2^0 , the Hill coefficient of the transfer is $H = N(\gamma^{J/2} - 1) / (\gamma^{J/2} + 1)$ where $\gamma = \exp -(\delta F_1^0 + \delta F_2^0) / RT$. Unlike the case of homogeneous binding a high value of H is best ensured by a high value of N . In agreement with these predictions, the transfer of bovine serum albumin from water to butanol by addition of Na p-toluenesulfonate at pH 2.4 yields $H \sim 28$. This value is in agreement with the high number of binding sites. Experiments to characterize the protein-ligand complex in the upper phase are also discussed.

F-POS-K15 PREDICTION OF HYDRODYNAMIC PROPERTIES OF GLYCOSAMINOGLYCANS IN DILUTE AQUEOUS SOLUTION. R. Potenzzone, Jr. and A.J. Hopfinger, Department of Macromolecular Science, Case Western Reserve University, Cleveland, Ohio, 44106

For Glycosaminoglycans (GAG), hyaluronic acid (HA), chondroitin-6-sulfate (C6S), chondroitin-4-sulfate (C4S) and dermatan sulfate (DS) have been subjected to our conformational analysis using Molecular Mechanics. The effects of hydration have been incorporated in our calculations. Limiting physico-chemical states, e.g. uncharged and charged forms, have been studied so that end points in pH and ionic strength titrations could be examined. The effect of high concentrations of Na^+ have also been included in our models. The partition function has been approximated and the related probabilities for the conformational states were calculated for each physico-chemical form. From this information along with Monte Carlo sampling methods $\langle R_g^2 \rangle$ values have been predicted. The corresponding chain statistics will be presented and compared to available experimental hydrodynamic data.

F-POS-K16 INTERACTIONS OF TYPE II COLLAGEN AND GLYCOSAMINOGLYCANS. D. C. Brooks* and J. Blackwell, Department of Macromolecular Science, Case Western Reserve University, Cleveland, Ohio 44106.

Collagen interacts with glycosaminoglycans at acid pH such that the thermal stability of the collagen triple helix is increased. In previous work using circular dichroism spectroscopy, we have shown that different proportions of the various common glycosaminoglycans are necessary to achieve maximum elevation of the melting temperature for calf skin collagen, which is a mixture of collagen types I and III. We have now studied the interactions of type II collagen (from pig laryngeal cartilage) with chondroitin 4- and 6-sulfates, keratan sulfate, and heparin. The results indicate that lower proportions of glycosaminoglycans are necessary for maximum interaction with type II collagen than with skin collagen, although the limiting thermal stability is the same in both cases. These studies are being extended to include purified types I and III collagens and conditions of physiological pH and ionic strength.

F-POS-K17 QUASI-ELASTIC LIGHT SCATTERING STUDIES OF POLYPEPTIDE-GLYCOSAMINOGLYCAN INTERACTIONS. K. P. Schodt, M. E. McDonnell, A. M. Jamieson, and J. Blackwell, Department of Macromolecular Science, Case Western Reserve University, Cleveland, Ohio 44106.

Quasi-elastic light scattering studies have shown that large multimolecular aggregates are formed on mixing dilute aqueous solutions of cationic polypeptides and anionic glycosaminoglycans. Translational diffusion coefficients calculated from the half-widths of the scattered Rayleigh spectra were used to determine the effective radii for the interacting systems. For equimolar-residue proportions of poly(L-lysine) and chondroitin 6-sulfate at a total concentration of 0.176mg/ml, the aggregates had average radii of 115nm. Circular dichroism spectroscopy has shown that addition of the glycosaminoglycan induces a conformational change in the polypeptide from the coil form to the α -helix, a change which can be reversed by raising the temperature above 47°C. Only slight changes in the radius are observed during this transition, indicating that the aggregates remain intact. Angular dependence studies give information on the shape of the aggregates. In addition, changes in the mixing-ratio, pH, and ionic strength produce changes in the size of the aggregates.

F-POS-K18 AGGREGATION REACTIONS AND T7 DNA BINDING OF E. COLI RNA POLYMERASE, C. G. Wensley*, H. S. Strauss*, R. R. Burgess* and M. T. Record, Jr., Department of Chemistry and McArdle Laboratory, University of Wisconsin, Madison, Wisconsin, 53706.

We are investigating the aggregation reactions of core and holo forms of RNA polymerase as functions of monovalent and divalent cation concentration by boundary sedimentation velocity. Our results confirm and extend the investigations of Berg and Chamberlin (*Biochemistry* 9, 5055-5064 (1970)) and indicate that Mg^{++} has a dramatic effect (at 0.01M) on the extent of aggregation attained at low ionic strength. We are also studying the specific and nonspecific interactions of RNA polymerase with intact T7 DNA by differential sedimentation velocity and nitrocellulose filter binding assays, as functions of temperature, pH, and monovalent and divalent ion concentrations. In the absence of divalent cations, all polymerase-DNA interactions show an extreme salt dependence, which indicates that ion pair formation makes a substantial contribution to the binding free energy (Record, Lohman, and deHaseth, *J. Mol. Biol.* 107, 000 (1976)). (This investigation is supported by funds from the NSF and NIH.)

F-POS-K19 MECHANISM OF TOBACCO MOSSAIC VIRUS (TMV) SELF ASSEMBLY. S. J. Shire, J. S. Steckert*, M. Adams* and T. M. Schuster, Biological Sciences Group, University of Connecticut, Storrs, CT 06268.

Previous studies in phosphate buffer pH 7.0 $\mu=0.1M$ at 20° have been equivocal concerning the role of the 4S and 20S disk aggregate in the elongation phase of the TMV self assembly reaction (K. Richards & R. Williams, *Comprehensive Virology* 6, 1 (1976)). These authors suggest that the ambiguity arises from the presence of both protein species during reconstitution and their rapid interconversion under the conditions used. We have recently investigated conditions (Shire, Steckert & Schuster, *Biophysical Journal* 16, 95a (1976)) at pH 6.5 in phosphate buffer, $\mu=0.1M$ and 6.5°C where the 20S species exists in a metastable state (~50% 4S & 50% 20S) and decays with a half-time of ~11 days to its equilibrium state (~98% 4S & 2% 20S). This ~20S species is capable of nucleating TMV-RNA under the metastable conditions. Moreover, the rate of reconstitution is slower under these conditions than at pH 7.0, 20°C and this has enabled us to monitor with analytical ultracentrifugation and electron microscopy the rate of disappearance of the 20S and 4S species as well as the appearance of growing TMV rods. The essential features of the reconstitution at pH 6.5, 6.5°C, TMV protein: RNA at 20:1 are as follows: (1) at early time (within the first 30 minutes) a 90S species appears which over time develops into three major peaks of ~90S, 120-130S and 168S, which all slowly convert to the 168S peak (87% by weight of the entire reconstitution peak) and (2) within the first 5 hours of reconstitution the 4S species incorporates at least 2 to 3 times more rapidly, on a molar basis, than the 20S disk species.

Supported by NIH Grants AI-11573 and AI-05266.

F-POS-K20 A STRUCTURE AND FUNCTION MODEL FOR COUPLING BETWEEN REGULATORY AND ACTIVE SITES. A. Bennun, Department of Zoology, Rutgers University, Newark, N. J. 07102.

A single divalent metal coordinates with up to six R-groups containing negative atoms from different or the same polypeptide chains, allowing specific chain foldings and/or monomeric subunits to arrange themselves within polymeric protein structures. Allosteric modulators capable of competitive chelating effects may be able to change the strength of interaction between the subunits of a polymeric structure, and/or those which maintain the folding of subunits. This effect may involve, reversibly, competitive effects changing from hexa to tetra or bidentate the coordinative number maintained by the protein's R-groups and/or the membrane's phospholipids negative atoms which are surrounding the divalent metal. This modulator-dependent modification of the number of R-groups, or the substitution of one R-group by others within the structure, includes various possibilities such as the modulator facilitating the reorganization of a tetradentate chelate structure from planar to tetrahedral coordination. It is proposed that the allosteric site of some regulatory enzymes may not be other than a modulator-modifiable chelate structure. An analogous coupling mechanism has been described (Bennun, A., 1975, *Biosys.* 7, 230) by proposing that hemoglobin's β -92 histidine is capable to compete with oxygen for only one of the six coordinative positions of the iron atom within the haem structure. However, β -92 histidine may, alternatively, coordinate to Mg^{2+} jointly with β -93 cysteine and other R-groups known to change in their reactivity, such as β -143 histidine. Bohr's protons and organic phosphates by competitively releasing β -92 histidine from its coordination with Mg^{2+} may therefore play the role of negative modulators. Zn^{2+} stabilizes a chelate structure and it is known to increase by three fold hemoglobin's oxygen affinity, but it may, therefore, desensitize its response to modulators.

F-POS-K21 THE PRECISE DETERMINATION OF THE WHOLE BLOOD OXYGEN EQUILIBRIUM CURVE. R. M. Winslow*, M. Swenberg*, R.L. Berger, R.I. Shrager*, M. Luzzana*, M. Samaja*, and L. Rossi Bernardi*, Molecular Hematology Branch, Laboratory of Technical Development, NHLBI, NIH, Bethesda, Md. 20014, and University of Milan, Milan, Italy.

Investigation of the effects of H^+ , CO_2 , 2,3-DPG, and other effectors on Hemoglobin (Hb) function has been fruitful because of the availability of methods for the measurement of the oxygen equilibrium curve (OEC) of Hb solutions at extremes of saturation. Studies with whole blood, however, have been limited by the unavailability of methods of equal precision and which are rapid enough to preserve cell constituents. p50 measurements (measures of the position of the OEC) are useful for clinical screening, but do not provide information about the shape of the OEC. We have previously described (1) a method for the measurement of the middle portion of the blood OEC (1-150 mm Hg) by the addition of H_2O_2 to deoxygenated blood containing catalase. We have now extended the observation to include the pO₂ ranges 0.1-1 mm Hg, and 150-650 mm Hg by relatively simple mixing methods. The curve (pH 7.4, pCO₂ = 40 mm Hg, 37°) thus determined lies slightly to the right of the standard curve of Rougfont. The greatest difference is at low saturation, probably owing to the fact that the latter data were obtained under conditions which would lead to depletion of cellular 2,3-DPG. The range of p50 values for 4 normal subjects was 28.3 - 29.0 mm Hg. The 4 constants for Adair's oxygenation scheme can be easily derived by digital computer. These constants are very sensitive to changes in the shape of the OEC, and are much more useful than p50 measurements in the investigation of the various allosteric effectors of Hb function within the red cell. Moreover, this analysis allows investigation of the OEC in the physiological-ly important range of 40-100 mm Hg.

1. L. Rossi-Bernardi, et. al., *Clin. Chem.* 21, 1747, 1975.

F-POS-K22 THE FOLDING OF COBALT-CARBONIC ANHYDRASE. L.M. McCoy* and K.P. Wong , Department of Biochemistry, University of Kansas Medical Center, Kansas City, Kansas 66103.

Cobalt carbonic anhydrase B from bovine erythrocyte can be prepared by replacing the Zn(II) in the native protein by Co(II) with almost complete retention of enzymic activity. As a continuation of our studies on the mechanism of folding of carbonic anhydrase [Wong, K.P., and Tanford C., *J. Biol. Chem.*, 248, 8518 (1973); Wong, K.P. and Hamlin, L.M., *Arch. Biochem. Biophys.*, 170, 12 (1975)], we have attempted to elucidate the mechanism of the acquisition of active site conformation by studying the unfolding and refolding of cobalt carbonic anhydrase, since it possesses characteristic absorption and circular dichroism spectra in the visible region which reflects primarily the local conformational environment of the active site where the Co(II) is bound [Coleman, J.E., *Inorg. Biochem.*, 1, 488 (1973)]. The conformation of the cobalt-protein is found to be almost the same as the native zinc-protein. The cobalt-protein has lower thermal stability and unfolds at a lower concentration of guanidine hydrochloride even though a single-phase transition is observed in these denaturations. The unfolding to the random coiled protein was monitored by various optical methods which reflect different conformational changes. The results show that separable stages of unfolding are observable for the cobalt-protein. It appears that the collapse of the active site conformation as monitored by changes in visible absorption and circular dichroic changes occurs immediately after the loosening of the molecule. This is followed by the exposure of buried aromatic residues and the unravelling of the secondary structures. However, refolding of the cobalt-protein results in an inactive renatured protein which has optical properties significantly different from the native cobalt-protein. [Supported by NIH Grants (HL-18905 and GM-22962).]

F-POS-L1 CYTOCHROME OXIDASE-OXYGEN KINETICS AT -100° : IS THERE AN OXYGEN POCKET? B.Chance
Johnson Research Foundation, University of Pennsylvania, Philadelphia, PA 19174

Flash photolysis of cytochrome oxidase-CO in the presence of oxygen at -100° involves no detectable electron transfer in the first few seconds of the reaction and leads to the formation of compound A, oxy-cytochrome oxidase $\text{Fe}_2^{2+}\text{Fe}_2^{3+}\text{Cu}_2^{2+}\text{O}_2$ (1). Remarkably, the equilibrium of O_2 and a_3^{2+} can be demonstrated at -100° ($K_D = 320 \mu\text{M}$ at -94°). This is supported by the linearity of the pseudo first order constant and the $[\text{O}_2]$ over a range of 0.05 to 3 mM at -94° and 0.07 to 0.7 mM at -105° indicating a bimolecular reaction in the active site of the enzyme. Proton NMR measurements show freezing of water protons to be complete between -50° and -80° (2). The second order constant follows Arrhenius' equation ($E_A = 9.9 \text{ Kcal/mole}$ from -20° to -110°). Postulation of an oxygen pocket near $\text{Fe}_2^{2+}\text{Fe}_2^{3+}\text{Cu}_2^{2+}$ that has an O_2 capacity sufficient to simulate the solution concentrations at the temperature of O_2 addition and trapping (-22°) seems required. Parallel studies on detergent solubilized cytochrome oxidase shows similar equilibria and second order reaction kinetics (3). Thus the membrane structure may not constitute an oxygen pocket, while the cytochrome oxidase protein may do so. These results identify striking differences between the reactions of O_2 and CO and between cytochrome oxidase and myoglobin (4).

- 1) B. Chance, et al, J. Biol. Chem. 250:9226-9237 (1975).
- 2) J.S. Leigh, personal communication.
- 3) C. Saronio, personal communication.
- 4) See other abstracts on Low Temperature Molecular Biophysics.

F-POS-L2 EFFECT OF MEMBRANE ENERGIZATION ON THE BINDING OF CO AND OXYGEN BY MITOCHONDRIAL CYTOCHROME c OXIDASE AT LOW TEMPERATURES. H.J. Harmon and M. Sharrock, Department of Biochemistry and Biophysics, University of Pennsylvania, Philadelphia, PA 19174

Energization of pigeon heart mitochondria by ATP addition results in the acceleration of recombination of the enzyme with CO following flash photolysis and acceleration of oxygen intermediate formation following photolysis in the presence of O_2 at low temperatures (1). The rate of oxygen binding as a function of oxygen concentration at -116°C was studied in both energized and FCCP-uncoupled samples. The acceleration of oxygen binding upon energization is readily apparent only at oxygen concentrations in excess of 200 μM . In the presence of FCCP, the rate of oxygen binding is independent of oxygen concentration. Similar results are seen in CO-binding experiments. Following flash photolysis at temperatures down to -95°C , energized mitochondria show accelerated kinetics in the presence of 100 and 1000 μM CO. This acceleration is most pronounced at low temperatures. In the presence of 10 μM CO, no differences between the energized/de-energized samples are observed. As in the case of isolated cytochrome oxidase (2), biphasic kinetics are observed at low CO concentrations. The slower phase may represent binding of molecules from the solvent while the fast phase represents the binding of molecules from a site nearer the heme. This suggests that the acceleration in mitochondria may be a result of altered membrane permeability for the ligand or a different binding capacity (other than that of the heme site) for the ligand.

- 1) Harmon, H.J., Chance, B., and Wikstrom, M.K.F., Biophysical J. 16, 13a, 1975.
- 2) Sharrock, M. and Yonetani, T., Abstracts, this meeting.

(Supported by NIH Grants GM01997-02, GM12202, HL14508 and NSF BMS73-00970.)

F-POS-L3 LOW-TEMPERATURE CO-BINDING AS A PROBE OF CYTOCHROME OXIDASE ENVIRONMENT.

M. Sharrock and T. Yonetani, Department of Biochemistry and Biophysics, University of Pennsylvania, Philadelphia, PA 19174

Low-temperature CO-binding by the cytochrome a_3 of isolated beef-heart cytochrome oxidase has been studied by flash photolysis in frozen aqueous solutions of potassium phosphate buffer and nonionic detergent (Tween 20). Between -10° and -40° and at low CO concentrations ($\leq 10 \mu\text{M}$), binding is biphasic and follows second-order kinetics. The rate of each phase shows non-Arrhenius behavior as a function of temperature, probably because of physical changes in the surroundings of the protein. The rate of the fast phase decreases with increasing detergent concentration, but shows little dependence on the salt concentration of the buffer. The rate of the slow phase, in contrast, decreases with increasing salt concentration and has only a secondary dependence on detergent. These effects are lost below -40° and at temperatures near or above 0° . Our results suggest that the cytochrome oxidase molecules are aggregated in micelles of detergent and possibly protein-bound lipid. CO molecules that remain within the micelle after photolysis rebind quickly; those that diffuse out into the solvent rebind more slowly. Both the micelles and their solvent surroundings appear to retain some fluidity down to approximately -40° . This system may be useful as a model for understanding the interaction of cytochrome oxidase with the mitochondrial membrane, and can be related to current work on membrane energization (1) and oxygen binding (2).

Supported by NIH grant HL 14508 and NSF grant BMS 73-00970.

- (1) H.J. Harmon and M. Sharrock, these abstracts
- (2) B. Chance, these abstracts

F-POS-L4 LOW TEMPERATURE BIOMOLECULAR PHYSICS I. MULTIPLE BARRIERS. N. Alberding, R.H. Austin*, S.S. Chan, L. Eisenstein, H. Frauenfelder, I.C. Gunsalus*, T.M. Nordlund* and A.H. Reynolds* Departments of Physics, Biophysics and Biochemistry, University of Illinois, Urbana, IL 61801.

Kinetic measurements of ligand (CO and O₂) binding to heme proteins and model compounds have been performed over wide ranges in temperature (2-340 K) and time (10⁻⁶ to 10³ sec) using flash photolysis. Myoglobin, separated α and β chains of hemoglobin, carboxymethylated cytochrome *c*, cytochrome P450 with and without substrate camphor, and model compounds protoheme and heme *c* octapeptide have been studied. Binding to all these heme proteins and compounds exhibits several distinct processes. At temperatures above 300 K a ligand-concentration and solvent-dependent process dominates, while below about 180 K rebinding is independent of ligand concentration and nearly insensitive to solvent. Between 180 and 300 K, the proteins, but not the model compounds, exhibit additional kinetic regions which depend upon protein and ligand. We describe these kinetics by assuming that a ligand moving from the solvent to its heme binding site encounters several Gibbs energy barriers: the outermost is formed by the solvent or solvent interface, the innermost by the heme group itself and the intermediate ones by protein structure. At low temperatures, flash photolysis probes the inner barrier and structure near the active center; at higher temperatures, barriers controlling access to the heme contribute to the kinetics. By fitting the observed time dependence of the data at all temperatures, the enthalpy, entropy and Gibbs energy changes at the barriers are determined. Correlations of the results with known structural features of the heme proteins and model compounds are made. Supported in part by NIH grant GM 18051 and NSF grant BMS 74-01366.

F-POS-L5 LOW TEMPERATURE BIOMOLECULAR PHYSICS II. DISTRIBUTED ENTHALPY AND ENTROPY. N. Alberding, R.H. Austin*, S.S. Chan, L. Eisenstein, H. Frauenfelder, I.C. Gunsalus*, T.M. Nordlund* and A.H. Reynolds* Departments of Physics, Biophysics and Biochemistry, University of Illinois, Urbana, IL 61801.

At temperatures below about 180 K, one common process is observed in the rebinding of ligands to heme proteins and model compounds. This process is independent of ligand concentration and to good approximation follows a power law of the form $(1 + t/t_0)^{-n}$ where t_0 and n are temperature-dependent parameters. The nonexponential behavior can be explained by assuming that the innermost barrier is characterized not by a unique value of the activation enthalpy but by an enthalpy distribution. The distributions have been determined from the measured time and temperature dependences of the rebinding, assuming that for a given activation enthalpy the rate follows the Arrhenius law. The distributions, which are different for each compound, appear to be a property of the heme which is influenced by the protein structure. The existence of different conformational states, each with a different activation enthalpy for the final rebinding step at the heme, may explain the observed distributions. For heme proteins the data can be fitted with a single-valued activation entropy. For heme model compounds, however, the activation entropy is also found to be distributed and linearly related to the enthalpy. Supported in part by NIH grant GM 18051 and NSF grant BMS 74-01366.

F-POS-L6 LOW TEMPERATURE BIOMOLECULAR PHYSICS III. MOLECULAR TUNNELING. N. Alberding, R.H. Austin*, S.S. Chan, L. Eisenstein, H. Frauenfelder, and T.M. Nordlund* Departments of Physics and Biophysics, University of Illinois, Urbana, IL 61801.

Rebinding of carbon monoxide to heme proteins and model compounds follows the Arrhenius law corresponding to classical over-the-barrier motion above 20 K; below, the rebinding becomes temperature independent, implying tunneling. Quantum mechanical tunneling and the Arrhenius process are both described by an enthalpy spectrum. The spectrum is determined from the data in the temperature range where binding occurs over-the-barrier. We assume that the tunneling barrier is described by the same spectrum. Tunneling then provides additional information about the nature of the barrier, including its width. To extract the barrier width from the observed tunneling rate, the mass of the tunneling particle must be known. We postulate that the binding process corresponds to the simultaneous motion of the Fe and CO toward the heme plane and take the mass to be the reduced mass of Fe and CO. We find that the barrier width, $d(H)$, depends on the activation enthalpy and that a fit to the data can be obtained with $d(H) = (H/H_{\text{peak}})^{\delta} d_0$, where H_{peak} is the enthalpy at which the distribution peaks. For a parabolic barrier we obtain values of $d_0 = .05 \pm .01$ nm and $\delta = 1.5 \pm 0.4$ for the separated β chain of hemoglobin and $d_0 = .03 \pm .01$ nm and $\delta = 1.4 \pm 0.4$ for protoheme.

Supported in part by NIH grant GM 18051 and NSF grant BMS 74-01366.

F-POS-L7 LOW TEMPERATURE BIOMOLECULAR PHYSICS IV. PRESSURE EFFECTS. N. Alberding, R.H. Austin, S.S. Chan, L. Eisenstein, H. Frauenfelder, and T.M. Nordlund, Departments of Physics and Biophysics, University of Illinois, Urbana, IL 61801.

Reactions can be completely characterized thermodynamically only if their behavior as a function of pressure as well as temperature is investigated. Preliminary measurements on CO binding to myoglobin and protoheme at pressures up to 2 kbar in the temperature range 60 to 300 K have been performed. Experiments fall into three categories: 1) Pressurizing with helium gas when the solvent is fluid. Large effects on the reaction rates are observed and activation volumes for the various processes determined. For myoglobin, high pressure causes the activation enthalpy spectrum to broaden and shift toward lower enthalpies. 2) Pressurizing with helium gas when the solvent is solid. Reaction rates are not measurably affected. 3) Using high CO concentrations (10 bar of CO pressure, for which hydrostatic pressure effects are minimal). Processes governed by barriers inside the protein become dependent on CO concentration, suggesting that more than one CO molecule is inside the protein.

Supported in part by NIH grant GM 18051 and NSF grant BMS 74-01366.

F-POS-M1 MEMBRANE COMPOSITION AND SURVIVAL OF IRRADIATED *E. COLI* K1060. M.B. Yatvin, J.J. Gipp*, and H.G. Sacks*, Radiobiology Laboratory, Departments of Radiology and Human Oncology, University of Wisconsin Medical School, Madison, Wis. 53706.

A fatty acid (FA) auxotroph of *E. coli* K1060 was used to study the effect of membrane composition and fluidity on survival after exposure to either ionizing or UV irradiation. The cells were supplemented with either linolenic, oleic, elaidic or palmitelaidic acid and the membrane FA composition verified by gas chromatography. Survival was determined on cells exposed to radiation above and below the transition temperature (Tt) (liquid crystal \rightarrow gel) of each FA. Survival was comparable for cells γ -irradiated and maintained for ~ 1 hour in the liquid-crystalline state prior to plating. When exposed at temperatures below the Tt (gel state), however, a significant decrease in survival was observed. In contrast, membrane fluidity did not influence the survival of UV irradiated bacteria. When the bacteria were consecutively substituted with 2 FA's differing in their Tt's and then irradiated below the Tt of one, survival corresponded with that obtained when the cells were grown entirely in the lower Tt fatty acid. This protection occurred even when the FA with the lower Tt was substituted during only 5% of a 100 min growth period. Damage and repair of a "DNA-membrane complex" is also correlated with the fluid state of the membrane during exposure to γ -irradiation. Irradiation below the Tt resulted in greater initial damage to the complex and less "repair" during the post-exposure incubation period. Thus, the membrane and its physical state play an important role in injury, "repair" and subsequent survival of bacterial exposed to γ -irradiation.

Supported in part by NIH Grant CA-16579 and NIH Center Grant CA-19278.

F-POS-M2 DNA DAMAGE AND "REPAIR" IN V79 CELLS IRRADIATED AS MONOLAYERS OR MULTICELL SPHEROIDS. R.E. Durand and P.L. Olive, Divisions of Radiation Oncology and Clinical Oncology, Wisconsin Clinical Cancer Center, University of Wisconsin Medical School, Madison, Wis. 53706.

Chinese hamster V79 cells can be grown as monolayers, or in suspension as multicell spheroids. When irradiated, cells from spheroids can accumulate more sub-lethal damage than cells from monolayers as evidenced by a wider shoulder on the survival curve. We have attempted to determine whether this increased resistance of spheroids to damage by ionizing radiation is reflected by DNA damage. The production and repair of single-strand breaks was quantified using alkaline sucrose gradient sedimentation and hydroxyl-apatite chromatography. Both methods indicated that equal amounts of radiation damage per rad were produced in cells grown as single cells or as spheroids, and that post-irradiation rejoining of 'breaks' also occurred with similar efficiency. Thus, these results suggest that the enhanced survival of cells irradiated as spheroids is dependent on processes other than (or in addition to) initial radiation damage to DNA.

F-POS-M3 ALTERNATIVE PATHWAYS FOR EXCISION REPAIR IN *ESCHERICHIA COLI*. Priscilla K. Cooper and Joyce G. Hunt*, Biology Department, Stanford University, Stanford, California 94305.

Excision repair of UV-induced damage to DNA in *E. coli* is initiated by a UV-endonuclease nick. Removal of the damage and resynthesis of the excised region by DNA polymerase I follows. Previous studies on mutants deficient in either polymerizing activity (*polA1*) or 5' \rightarrow 3' exonuclease activity (*polAex2*) of pol I have indicated that alternative enzymes can operate in both excision and resynthesis, resulting in lower survival after UV, increased DNA degradation, and longer repair patches (Cooper, MGG in press). We propose a model for these alternative pathways. In *polAex2*, resynthesis is performed by remaining pol I activity, while excision utilizes an alternative 5' \rightarrow 3' exonuclease, e.g. *exo VII* or the *recB,C* nuclease (*exo V*). Longer repair patches result from more extensive degradation and resynthesis in the 5' \rightarrow 3' direction. In *polA1*, excision and resynthesis is performed by pol II or III coupled with the remaining pol I 5'-exonuclease; since these polymerases require a gap for binding, the initial nick would have to be expanded by 3' \rightarrow 5' degradation. Longer repair patches would then result from resynthesis of this 3' \rightarrow 5' degradation and from increased synthesis after dimer removal. Reduced UV-induced degradation in *polA1recCts* mutants compared to *polA1* (Katsuki and Sekiguchi, BBA 383:188, 1975) implicates *exo V*. We are studying possible involvement of *exo V* in alternative pathways using a *recBtsrecCts* mutant, both alone and in combination with *polA1* or *polAex2* mutations. Additional presence of the *recB,C* mutations in a *polA1* mutant at the restrictive temperature does not prevent the increase in repair synthesis characteristic of *polA1* mutants but does appear to reduce dimer excision. If *exo V* does participate in gap expansion in *polA1* mutants, it is thus apparently not the only enzyme that can do so. The question of whether it can directly participate in dimer excision in the absence of polymerase I 5'-exonuclease activity is under investigation.

F-POS-M4 GENETIC AND MOLECULAR CHARACTERIZATION OF RADIATION-SENSITIVE MUTANTS IN *DICTYOSTELIUM DISCOIDEUM*. D. L. Welker* and R. A. Deering. Biophysics Program, Department of Biochemistry & Biophysics, The Pennsylvania State University, University Park, PA 16802

The haploid wild type strain (NC-4) of the cellular slime mold, *D. discoideum*, a model developmental system, is relatively resistant to ^{60}Co gamma rays, 254 nm ultraviolet light (UV), and alkylating agents. Several mutants more sensitive to one or more of these agents have been isolated, and assigned by parasexual analysis to at least four of the seven chromosomal linkage groups of this eukaryote. Those loci to be discussed here, *radA* (from γ s-20), *radB* (from γ s-13), and *radC* (newly isolated) map on linkage groups I, VI, and III, respectively. *RadA* and *radB* confer sensitivity to both UV and gamma rays, whereas *radC* makes the cells more sensitive to UV but not to gamma rays. In diploids constructed by fusion of haploids, the sensitive characteristic is recessive to the wild type for all three of these loci. Haploids with *radC* are defective in an endonuclease that yields single strand breaks in the nuclear DNA after UV irradiation, as determined by alkaline sucrose gradient analysis. *RadB* allows the wild type level of post-UV strand breakage and dimer excision but yields a slower rate of strand rejoining (Guialis & Deering, *J. Bacteriol.* 127, 59 (1976)). A haploid strain bearing both the *radA* and *radC* mutations is more sensitive than either the *radA* or *radC* haploid, indicating that these mutations are in different repair pathways. The *radA* and *radB* genes seem to be in the same pathway since a *radAradB* double mutant haploid has the same sensitivity as the *radB* haploid. These results indicate that the cells of this organism are capable of DNA repair by at least two pathways and that mutations located on several chromosomes can alter various steps in these pathways. (NIH GM 16620).

F-POS-M5 THE EFFECT OF CAFFEINE ON THE SURVIVAL OF HeLa S3 CELLS AS A FUNCTION OF X-RAY DOSE AND CELLULAR AGE. P.M. Busse,^{1,2*} S.K. Bose,² R.W. Jones,^{1*} and L.J. Tolmach,¹ Dept. of Anatomy, Washington University School of Medicine, St. Louis, Mo. 63110,¹ and Dept. of Microbiology, St. Louis University School of Medicine, St. Louis, Mo. 63104.²

Post-irradiation treatment of HeLa S3 cells with 1 mM caffeine results in a marked diminution of the surviving fraction as scored by colony formation. The decrease is dose dependent: the predominant effect of a 24-hour post-irradiation treatment of a non-synchronous population with caffeine is to reduce the slope of the survival curve (D_0) from 130 to 60 rad. The shoulder is also slightly reduced, but is not completely removed. The amount of post-irradiation killing is maximal if cells are exposed to caffeine at a concentration of at least 1 mM for 12 hours. No unirradiated cells are killed under these conditions. Dose-response curves were also obtained for synchronous cells at various phases of the cell cycle. Similar results were obtained at all cell ages, but the magnitude of the effect is age-dependent. This age dependence was further explored in experiments in which mitotically collected cells were exposed to 300 or 500 rad doses at 2-hour intervals throughout the cell cycle. Treatment with caffeine for 24 hours after irradiation enhances the killing of cells in S phase more than cells in G1. Caffeine-induced expression of the potentially lethal x-ray lesion(s) can be initiated as late as 12 hours after irradiation. There appears to be some overlap between the lesions affected by caffeine and those with which hydroxyurea interacts.

F-POS-M6 N-ACETOXY-2-ACETYLAMINOFLUORENE INHIBITS REPAIR OF DAMAGED DNA IN CHINESE HAMSTER CELLS. F.E. Ahmed, and R.B. Setlow, Biology Department, Brookhaven National Laboratory, Upton, N.Y. 11973

Normal human fibroblasts are able to repair DNA damaged by UV and N-acetoxy-2-acetylaminofluorene (AAAF) whereas xeroderma pigmentosum cells lack these abilities. We showed earlier that the amount of repair in normal human fibroblasts from a combined treatment was additive. Chinese hamster (V-79) cells have a much lower capacity to perform excision repair of UV damage than human fibroblasts. Hence, we wished to determine the ability of these cells to perform excision repair of AAAF damage and repair as a result of a combined treatment with UV and AAAF. The techniques used to measure repair were: a) unscheduled DNA synthesis measured radioautographically, b) the photolysis of BrdU incorporated into parental DNA during repair, and c) the loss of sites sensitive to UV-endonuclease. We used an endonuclease from *M. luteus* that acts on pyrimidine dimers but does not act on AAAF-treated DNA to measure sites in DNA extracted from treated cells. Radioautographic data showed that the extent of repair after the combined treatment was much less than the sum of the two treatments separately at the lowest doses used (2.5 Jm^{-2} UV and $2.5 \mu\text{M}$ AAAF). BrdU photolysis studies showed that repair of AAAF damage in V-79 cells was of the UV type (long) and that repair after the combined treatment was much less than the sum of the two treatments at doses of 3.6 Jm^{-2} UV and $5 \mu\text{M}$ AAAF. The assay of UV-endonuclease sensitive site showed that a dose of $5 \mu\text{M}$ AAAF caused a ~35% inhibition of removal of sites arising from a dose of 2.5 Jm^{-2} UV. Therefore we conclude that the amount of repair is not additive and hence different from human cells and that AAAF does inhibit UV repair in V-79 cells. (Supported by U.S. Energy Research and Development Administration.)

F-POS-M7 ISOLATION OF UV-SENSITIVE VARIANTS OF CHO-K1 BY NYLON CLOTH REPLICA PLATING. T.D. Stamato, and C.A. Waldren*, Eleanor Roosevelt Institute for Cancer Research and the Department of Biophysics and Genetics, University of Colorado Medical Center, Denver, Colorado. 80262

Techniques are described which permit the identification and isolation of UV sensitive variants from mutagenized populations of Chinese Hamster Ovary (CHO) cells. Identification is based on the observation that within two days after receiving a large exposure (> 240 ergs/mm², 99% loss of CFA) of UV irradiation, colonies of CHO cells detach from the surface of a plastic tissue culture dish. Survival is defined in terms of colony forming ability (CFA). At a low dose of UV light (20 ergs/mm², 25% loss of CFA) which does not reproductively inactivate or detach a significant number of parental cells, UV sensitive colonies dislodge to produce a clear plaque in a lawn of unirradiated cells. Live cells from UV sensitive colonies are recovered from a nylon cloth replica prepared prior to irradiation. One sensitive variant (CHO-UV1) is indistinguishable from the parental cell in x-ray sensitivity, chromosome number, generation time, and duration of the phases of the cell cycle. However, the CHO-UV1 cell has a mean lethal dose (D_{01}) and shoulder width of the survival curve of 18 ergs/mm² and 27 ergs/mm², respectively, which are approximately half those of the parental cell. The above characteristics have remained unchanged for a period of seven months in culture. (Supported by F.D.A. Contract No. 222-75-2029(C). T.D.S. was supported by N.I.H. Fellowship No. 5F22 CA-02569).

F-POS-M8 5'→3' THYMINE DIMER EXCISING NUCLEASES IN CULTURED HUMAN CELLS. K.H. Cook,* and E.C. Friedberg, Laboratory of Experimental Oncology, Department of Pathology, Stanford University, Stanford, Ca. 94305

Three deoxyribonuclease activities from human KB cells have been identified and partially purified and characterized. All three activities utilize as a substrate UV-irradiated *E. coli* DNA that has been specifically incised on the 5' side of the dimer by preincubation with phage T4 UV endonuclease. The activities therefore excise dimers in the 5'→3' direction. The three activities are assayed by measuring the loss of thymine dimers from [³H] thymine-labeled DNA using a one dimensional thin-layer chromatographic system (1).

Each activity has been purified approximately 100 fold. The three activities are distinguishable on the basis of their relative affinity for DEAE-cellulose and phosphocellulose. Each activity can also be distinguished with respect to the optimum concentration of divalent cation required, effect of monovalent cations, sensitivity to SH-group inhibitors, isoelectric point and sedimentation coefficient. Preliminary studies indicate that none of the activities degrade double-stranded unincised DNA and only two of the three activities attack single-stranded UV-irradiated DNA. Thus one of the enzymes may be a single-strand specific endonuclease.

References

1. Cook, K.H. and Friedberg, E.C. *Anal. Biochem* **73**, 411-418 (1976)

Studies supported by research grants from the USPHS (CA-12428) and A.C.S. (NP 174) and by contract with the USERDA (E-(04-3)-326).

F-POS-M9 APPLICATION OF CT SCANS IN THE RADIATION (Co⁶⁰) THERAPY FOR BODY INHOMOGENEITIES. R.S. Ledley, L.S. Rotolo*, and S.H. Joseloff*, National Biomedical Research Foundation, and Medical Computing & Biophysics Division, Physiology & Biophysics Department, Georgetown University Medical Center, Washington, D.C. 20007

Three methods of correction have been developed to calculate the dose distribution for tissue inhomogeneities in radiotherapy, namely the effective attenuation μ method, the empirical displacement method, and the tissue/air ratio method. However, no method exists for corrections of arbitrary shapes of inhomogeneous tissues of bone, lung, and muscle. The difficulty here is the lack of information about the contours of inhomogeneous tissues. Using the ACTA-Scanner system, which provides the exact contours of inhomogeneities, the correct solution for this problem can be found. This paper describes a self-contained, on-line therapeutic planning system, used in conjunction with the ACTA-Scanner. The system is presently being used for radiation therapeutic planning on patients who have had ACTA scans.

F-POS-M10 EVALUATION OF MASS DENSITIES OF BODY TISSUES AND CALCIUM CONCENTRATIONS OF BONE BY COMPUTERIZED TOMOGRAPHIC TECHNIQUES. H.K. Huang, L.S. Rotolo*, and R.S. Ledley, National Biomedical Research Foundation, and Medical Computing & Biophysics Division, Physiology & Biophysics Department, Georgetown University Medical Center, Washington, D.C. 20007

The two methods described in this paper, one *in vivo* and the other *in vitro*, correlate CT (computerized tomographic) numbers with mass densities in a cross-sectional scan and CT numbers with the calcium concentration in bones. The *in vivo* method is based on patient scan results and theories used in computerized tomography, specifically the concept of average effective energy (AEE) and the Convolution Method in picture reconstruction. The *in vitro* method is based on scans of fresh excised lumbar vertebrae and on the physical analysis (by conventional methods) of the cancellous bone from the vertebrae. The *in vivo* method gives a good correlation for soft tissues and a quite reasonable one for bones. Since the definition of bone density is still quite controversial, an *in vitro* experiment was used to correlate the calcium concentration of bones with their CT numbers. The results will enable a more precise definition of bone density to be determined. The mass density distribution in a cross section can be used to plan radiation therapy and to create a data base for biomechanics research. A knowledge of the level of the calcium concentration in bones would also offer a significant diagnostic value in orthopaedics.

F-POS-M11 DETECTION OF DNA DAMAGE IN MAMMALIAN CELLS USING A NUCLEASE FROM PSEUDOMONAS BAL-31. S. Rosanky*, D. Vizard, and R. Meyn, Department of Physics, The University of Texas System Cancer Center, M. D. Anderson Hospital and Tumor Institute, Houston, Texas 77030

Radiation and chemically induced DNA damage have been detected in cultured mammalian cells using an *in vitro* enzymatic assay. The technique used was basically that of Paterson et al. (*Mutation Res.* 19(1973) 845). In this case, however, instead of the UV-specific endonuclease from *Micrococcus luteus* an enzyme from *Pseudomonas BAL-31* was employed. Gray et al. (*Nucleic Acids Res.* 2(1975) 1459) who originally isolated this activity, have reported that it has specificity for weakly hydrogen-bonded regions in DNA. Cultured Chinese hamster cells, prelabelled with ^{14}C -thymidine, were exposed to either ultraviolet light (UV) or N-hydroxy-2-acetylaminofluorene (N-OH-AAF). The DNA from the treated cells was isolated and purified, and then incubated at 50°C with the nuclease from BAL-31. The reaction was stopped by the addition of EDTA and the DNA was centrifuged for 17 hours at 16,500 rpm in a 5-20% alkaline sucrose gradient. The sedimentation profiles demonstrated that the BAL-31 nuclease recognized sites in the DNA generated by both UV and N-OH-AAF. Based on these data, this assay system appears sensitive enough to detect radiation or chemically induced damage in cells at significant (>10%) survival levels. This technique may, therefore, be a useful tool for the study of DNA lesions and repair in mammalian cells. Supported by Public Health Service Research grant number CA 04484 from the National Cancer Institute.

F-POS-M12 DIFFERENTIAL KILLING BETWEEN REPAIR DEFICIENT AND REPAIR PROFICIENT HUMAN CELL LINES AFTER EXPOSURE TO CARCINOGENS; APPLICATION AS A SCREENING TEST. Ann D. Burrell*, June J. Andersen*, and Erica S. Kay*, (Intr. by Charles Allen Smith), IBM Corporation, General Products Division, San Jose, Ca. 95193

We have developed a new method for comparing cell line responses to mutagens and carcinogens. The method is a mammalian version of the bacterial "repair test" and compares zones of killing between repair proficient lung fibroblasts (VA13 cells) and repair deficient xeroderma pigmentosum skin fibroblasts. Plates of nearly confluent cells are overlaid with 1% agar containing medium without phenol red, the test compound is applied to a well in the center of the plate and the plates incubated for 3 days. The zones of living cells are visualized by applying a further agar overlay containing 0.01% neutral red dye, and the killing zones are measured after 10-16 hours. Compounds which cause uv-mimetic damage, eg. 4-nitroquinoline oxide, show a greater zone of killing of the xeroderma pigmentosum cells than the normal cells. X-ray mimetic compounds, and toxic compounds which kill but do not damage the DNA, do not produce this enhanced sensitivity. UV-mimetic compounds which require activation by liver microsomal enzymes before they interact with DNA, eg. 2-amino anthracene can be detected by incorporating the S9 fraction used by Ames in the Salmonella test into the agar. The usefulness of the method as a screening test for chemical carcinogens should be analogous to the bacterial "repair test" after extension to include other cell lines, such as ataxia telangiectasia cells which show enhanced sensitivity to x-ray mimetic compounds. Two major advantages of the test are that it utilizes human cell lines and takes only 4 days to complete, compared to 14-21 days for the traditional mammalian cell mutagen studies.

F-POS-M13 ESR CHANGES IN CANCER: THE RELATIONSHIP BETWEEN FREE RADICALS FROM LYOPHILIZED AND NON-LYOPHILIZED TUMOR TISSUE. P.Gutierrez and H.Swartz, National Biomedical ESR Center, Dept. of Radiology, Medical College of Wisconsin, Milwaukee, Wisc. 53226.

There are conflicting reports on the free radical content of tissues during the growth of malignant tumors. A number of studies, usually using lyophilized samples, report an increase in free radical content during the early phases of tumor growth with a subsequent fall in concentration as the tumors become large. Studies in which the tumor tissues have been frozen but not lyophilized indicate that free radical concentrations decrease. There have not been any studies in which both methods of sample preparation were used on the same sample. Such an experiment could help resolve the apparent discrepancy in results and thereby permit an evaluation of the significance and usefulness of these findings. We wish to report the results of such a study. Walker 256 carcinoma was used because it has been reported to have a dramatic increase in free radical content during the early phases of tumor growth. The key finding is that while the intensities of the frozen gradually decreased as the tumors grew, these same samples, when lyophilized, had an increase in intensity similar to that previously reported. We did not observe a decrease at a later time in the signals from the lyophilized samples, in contrast with previous reports.

We tentatively conclude: 1. The increases observed with the use of lyophilized signals do not reflect *in vivo* levels of free radicals. 2. Growth of tumors may change the susceptibility of tissues to generation of free radicals by lyophilization, due to an increase in a precursor and/or a decrease in an inhibitor of the radical generating reaction.

F-POS-N1 CYTOCHROME *c* OXIDASE: REACTION WITH CO AND O₂. David F. Wilson and Yuriko Miyata,* Dept. of Biochemistry and Biophysics, University of Pennsylvania, Philadelphia, PA 19174.

The active site for reduction of O₂ to H₂O by cytochrome *c* oxidase contains cyt *a*₃ (E_m = 0.38V) and the "invisible copper" ²(E_m = 0.34V). In potentiometric titrations each titrates as a one electron acceptor (n=1.0) in the absence of added ligands. In the presence of 1 mM CO, an inhibitor competitive with respect to O₂, the reduced cyt *a*₃-CO compound titrates with an E_m of 0.43V and n=2.0 (Lindsay et al. 1975, A.B.B. 169, 492). Anaerobic suspensions of submitochondrial particles and isolated cytochrome oxidase were titrated reductively with NADH + phenazine methosulfate and oxidatively with molecular oxygen. Four equivalents per cytochrome *a* are required for complete reduction or oxidation of cytochrome oxidase. In the presence of CO (100 μM - 1 mM) two of the four equivalents are required for the formation of the reduced cytochrome *a*₃-CO compound as measured by the appearance of its characteristic absorption maximum at 590 nm. The measured absorbance change is proportional to the number of equivalents added or withdrawn throughout titration of the CO compound. These results demonstrate that reduction of cyt *a*₃ and the "invisible copper" occur with the same E_m in the presence of CO, in agreement with potentiometric analysis. Thus CO binds with high affinity only to the form of cytochrome oxidase in which both components are reduced. It is proposed that O₂ forms a bridged complex between the metal atoms and undergoes two electron reduction to bound peroxide followed by further reduction to H₂O. Supported by NIH GM 12202 and NIH GM 21524.

F-POS-N2 OXIDATION-REDUCTION COMPONENTS OF THE MITOCHONDRIAL CYTOCHROME *b-c* COMPLEX. M. Erecińska,* D.F. Wilson, and Y. Miyata,* Dept. of Biochemistry and Biophysics, University of Pennsylvania, Philadelphia, PA 19174. (Intr. by C.S. Owen).

A cytochrome *b-c*₁ complex was isolated from pigeon breast mitochondria and purified to a content of 3 μmoles of cytochrome *c*₁ per milligram of protein. The preparation was titrated under anaerobic conditions with reducing (NADH) and oxidizing (ferricyanide) equivalents. The oxidation-reduction components present in the preparation were determined by the number of reducing (or oxidizing) equivalents accepted (or donated) per cytochrome *c*₁ and compared with the stoichiometries of the known redox components measured by independent methods. The order of reduction or oxidation of the components was consistent with the known values of their half-reduction potentials, as determined by the potentiometric titration technique (Erecińska et al. 1973; Leigh and Erecińska 1975). The preparation donated (or accepted) 5.2 ± 0.3 equivalents per cytochrome *c*₁, while the measured content of cytochrome *c*₁, cytochrome *b*₅₆₁, cytochrome *b*₅₆₅, Rieske iron-sulfur protein, ubiquinone, and succinate dehydrogenase accounted for 5.0 ± 0.2 equivalents per cytochrome *c*₁. The conclusion is drawn that cytochrome *bc*₁ complex (energy transduction site 2), like cytochrome *c* oxidase (energy transduction site 3), contains four one-electron redox components: cytochrome *c*₁, cytochrome *b*₅₆₁, cytochrome *b*₅₆₅, and the Rieske iron-sulfur protein, present in stoichiometry 1:1:1:1. Supported by US PHS GM 12202.

F-POS-N3 CHARACTERIZATION OF THE CYTOCHROME *c* BINDING SITE IN MITOCHONDRIA USING METALLO-CYTOCHROME *c* DERIVATIVES. J.M. Vanderkooi and R. Landesberg,* Dept. of Biochemistry and Biophysics, University of Pennsylvania, Philadelphia, PA 19174.

The luminescence of iron-free, copper, tin and zinc cytochrome *c* and the electron paramagnetic resonance from copper cytochrome *c* have been used to characterize the interaction of cytochrome *c* with mitochondria. The fluorescence quantum yields of tin and zinc cytochrome *c* are not quenched when these derivatives bind to the mitochondria. Based upon spectral overlap and quantum yield, the distance between the porphyrin rings of cytochrome *a* and cytochrome *c* is calculated according to Förster's theory to be greater than 10 Å. At 77°K the fluorescence and phosphorescence emission spectra of Sn and Zn cytochrome *c* show evidence of resolution into vibrational bands, occurring at frequency differences 750 cm⁻¹ and 1540-1550 cm⁻¹ from the 0-0 transition. Measurement of the polarized emission of porphyrin and Zn cytochrome *c* bound to oriented layers of cytochrome *c* depleted mitochondria indicates that the heme plane is perpendicular to the plane of the membrane, although there is evidence that some of the molecules are randomly oriented. The luminescence of copper cytochrome *c* is characteristic of copper porphyrins in which unpaired metal d electron couples with the porphyrin triplet to give tripdoublet and quartet states. A difference in the emission spectra of mitochondrial bound and free copper cytochrome *c* can mean that a conformational change in cytochrome *c* occurs when it binds. The electron paramagnetic resonance spectrum of copper cytochrome *c* indicates that histidine is one ligand of the copper. Supported by NIH GM 12202.

F-POS-N4 PHOTODISSOCIABLE HYDROGEN ION BINDING TO BACTERIORHODOPSIN: EFFECT OF DETERGENT AND LIPIDS. Robert Renthal, Division of Earth and Physical Sciences, University of Texas at San Antonio, San Antonio, Texas 78285

Under steady illumination, the purple membrane (PM) of *Halobacterium halobium* attains an equilibrium of photo-intermediates, resulting in a small net acidification of the aqueous medium over a wide range of pH. I have measured the light-induced changes in proton binding to PM (Δh) at 20°C and 2×10^5 ergs/cm²sec intensity of 560 nm light under a variety of solvent conditions. In H₂O, Δh is less than 2 meq/mole between pH 5 and 7, and rises to about 30 meq/mole at pH 10. In 3 M NaCl or KCl, Δh is similar to that in H₂O below pH 7, but rises steeply above pH 8 to 65 or 150 meq/mole, respectively, at pH 9. In 0.1% Triton X-100, Δh is greater throughout the neutral pH region, and rises to a maximum of 80 meq/mole at pH 9. In 0.1% Triton and 3 M NaCl, there is a substantial increase in Δh at all pH, and the maximum increases to 160 meq/mole and shifts to pH 8. Chromatography of Triton-solubilized PM on hydroxyapatite separates bacteriorhodopsin (bR₅₇₀) from most of the phospholipid and glycolipid, as measured by organic phosphate analysis and periodate oxidation. The remaining protein, bR₅₅₀ (λ_{max} =550 nm), has an altered Δh , with the maximum occurring at pH 7. In terms of a simple 3-state model (protonated, dark; unprotonated, dark; and unprotonated, photo-excited) the results suggest that the apparent pK, in the dark, of the photodissociable hydrogen ion binding is greater than 10 in the intact membrane in H₂O. In Triton, under conditions where PM may be largely solubilized into monomeric protein-lipid subunits, the apparent pK is 9. After removal of lipid, the apparent pK is 7. The kinetics of light-induced proton release and uptake by bR₅₅₀ and by PM in salt and Triton are quite slow and resemble PM in salt and ether. (Supported by Research Corporation)

F-POS-N5 BINDING OF DIPROTONATED QUINACRINE MOLECULES TO ENERGIZED BEEF HEART SUBMITOCHONDRIAL MEMBRANES. Cheng-Schen Huang* and Chuan-pu Lee (Intr. by J. C. Bagshaw), Department of Biochemistry, School of Medicine, Wayne State University, Detroit, Michigan 48201

We have recently presented evidence indicating that the energy-linked fluorescence decrease of quinacrine (QA) associated with beef heart submitochondrial membranes results primarily from the protonation of monoprotonated QA molecules (QA·H⁺) with the formation of the diprotonated species (QA·2H⁺). QA·2H⁺ molecules are associated with the energized membranes in a fashion which prevents ready equilibration with the external medium (Biochim. Biophys. Acta, in press). The fluorescence polarization of QA associated with beef heart submitochondrial membranes at various metabolic states has been investigated. The degree of fluorescence polarization of QA was estimated to be 0.02, 0.10, and 0.20 for the system when QA molecules were alone or associated with submitochondrial membranes in the non-energized or energized state, respectively. The increase in fluorescence polarization of QA associated with submitochondrial membranes induced upon energization was observed at temperatures between 8 and 30°C, and in a medium with pH ranging from 7.2 to 8.2. Based on these data, together with the relative fluorescence quantum yields of QA molecules, an increase by a factor of 1.2 in the viscosity of the QA micro-environment associated with the energization of submitochondrial membranes was estimated. These data further substantiate our earlier contention that the diprotonated QA molecules are firmly bound to the energized submitochondrial membranes and that QA may serve as a convenient probe in estimating the H⁺ content in beef heart submitochondrial membranes induced upon energization (cf. Huang and Kopacz, Fed. Proc., 1977, in press). Supported by grants from the National Institute of Health (GM-22751) and the Muscular Dystrophy Association of America, Inc..

F-POS-N6 BIOCHEMICAL STUDIES OF SKELETAL MUSCLE MITOCHONDRIA OF MYODYSTROPHIC MICE.

C. P. Lee, M. Martens*, L. Jankulovska*, and M. A. Neymark*, Department of Biochemistry, School of Medicine, Wayne State University, Detroit, Michigan 48201

Myodystrophy, a new myopathy in the mouse caused by a spontaneous recessive mutation, was identified clinically and histopathologically by Lane and associates recently (J. Hered. 67, 135, 1976). We have made a systematic study of the biochemical properties of mitochondrial preparations isolated from skeletal muscle of myodystrophic mice (*myd*) and their normal littermates. Under optimal conditions the mitochondrial protein recovery (2 - 2.5 mg/g. tissue) of *myd* mice was comparable with that of controls. The cytochrome content of *myd* mitochondria was comparable with that of controls, with a content of 0.35, 0.34 and 0.56 nmoles/mg protein for cytochromes a, b and c (+c₁), respectively. The respiratory rates in State 3 with pyruvate + malate, or succinate (+rotenone) as substrates and the accompanying phosphorylation efficiencies of *myd* mitochondria were comparable with those of controls. However, the respiratory control ratio of *myd* mitochondria (3.4 ± 0.5) was consistently lower than that of controls (6.6 ± 0.6) with pyruvate + malate as substrates. A normal Ca⁺⁺ transporting capacity of *myd* mitochondria linked to succinoxidase was exhibited by *myd* mitochondria. With palmityl carnitine (+malate) as substrates the respiratory rate in State 3 of *myd* mitochondria was approximately 30% lower than that of controls, though the accompanying respiratory control and phosphorylation efficiency appeared to be comparable with those of controls. These data indicate that the *myd* mitochondria possess: (A) normal respiratory chain-linked oxidative phosphorylation and related activities; (B) a slight impairment of the fatty acid oxidative metabolism; and (C) a more delicate membrane than controls. Supported by a grant from the National Institute of Health, NS-08075.

F-POS-N7 CALCULATED EXCITATION PROFILES AND CLASSICAL NORMAL MODES OF HEMEPROTEIN RESONANCE RAMAN SPECTRA. L. Rimai and I. Salmeen, Engineering & Research Staff, Ford Motor Co., Dearborn, MI 48121

Resonance Raman spectra of heme proteins are discussed considering: (a) excitation profiles calculated from a simple D_{4h} model including two E_u excited electronic levels, their $n=0$ and $n=1$ vibrational sublevels, assumed B_{2g} vibrational coupling between degenerate E_u vibronic levels, and parameters estimated from optical absorption spectra; and (b) normal modes calculated classically from a simplified model for the four symmetry types of Raman active in-plane vibrations. These considerations lead to the classification of experimentally observed resonance enhanced fundamentals in terms of symmetry and specific atomic displacements. This classification applies to the high frequency region (above 700 cm^{-1}), dominated by conjugated bond stretches, and to the low frequency region (below 700 cm^{-1}), dominated by displacements of Fe-N bonds.

F-POS-N8 HEME PLANE ORIENTATION IN MITOCHONDRIAL MEMBRANES. J.S. LEIGH, Jr. and H.J. Harmon, Johnson Research Foundation, University of Pennsylvania, Philadelphia, PA 19174

Electron paramagnetic resonance spectra of cytochrome *c* oxidase and cytochrome *c* hemes in oriented multilayers have been investigated. Oriented multilayers prepared from sub-mitochondrial particles were studied with both cytochrome *c*-depleted and normal cytochrome *c*-containing preparations. The *g* 3.0 band of cytochrome *a* is observed only when the plane of the oriented multilayer is parallel to the magnetic field direction. "Dichroic ratios" of better than 10:1 are observed between parallel and perpendicular orientations. This indicates that the heme-normal direction (which is identified with the *g* 3.0 peak) is oriented exclusively in the plane of the membrane. Comparison of the normal and cytochrome *c*-depleted samples shows that the cytochrome *c* heme is similarly oriented. Oriented spectra from iron-sulfur proteins were also observed. With purified membranous cytochrome oxidase, the orientation dependence of the *g* 3.0 peak was virtually identical with that from oriented submitochondrial particles, implying that the heme orientation in the isolated state is similar to that in the mitochondrial membrane. Some differences in the orientation dependence of the *g* 2.2 region were noted, however. Oriented multilayers with cytochrome *c* oxidase-cytochrome *c* complexes show that both heme *a* and heme *c* are oriented with their heme-normals parallel to the membrane plane (heme planes perpendicular to the membrane plane).

F-POS-N9 A NEW MATHEMATICAL ANALYSIS METHOD OF MULTI-REDOX COMPONENT SYSTEMS. PROPERTIES OF THE *c*-TYPE CYTOCHROMES IN YEAST MITOCHONDRIA. M. Denis¹, E. Neau², J.P. Blein¹, I. Agali³ and P. Pajot³, (Intr. by M. Cohn), Laboratoire de Physiologie Cellulaire¹ et Laboratoire de Chimie Physique², U.E.R. Scientifique de Luminy, 13288 Marseille Cedex 2, France, Centre de Genetique Moleculaire³, 91190 Gif sur Yvette, France.

A direct relationship is achieved between absorbance and oxidation reduction potential: $A = \epsilon \cdot DA_0 [1 + \exp((E_m - E_h)/K)]^{-1}$. The properties of the observed components are defined by the spectrometric and potentiometric parameters fitted by the Newton-Raphson technique. The midpoint potential resolution limits of two components can be less than 5 mV by this new method. The computer analysis is able to yield individual difference spectra which would be impossible to obtain by direct means. Titrations were carried out with mitochondrial preparations from a wild type strain of *Saccharomyces cerevisiae* and a cytoplasmic respiratory deficient mutant lacking mitochondrial protein synthesis. Analyses of redox titrations at 552/542 nm have distinguished two midpoint potentials $E_{m1} = 257 \pm 4\text{ mV}$ ($n=1$) and $E_{m2} = 191 \pm 17\text{ mV}$ ($n=1$). The absorbance contribution of the species responsible for E_{m2} appears to be too weak to be attributed to cytochrome *c*₁. This component is assumed to be a *c*-type heme protein.

F-POS-N10 THE PROPERTIES OF MEMBRANE POTENTIAL INDICATORS IN NATURAL AND MODEL MEMBRANES.

C.L. Bashford[†]*, B. Chance[†], L.S. Powers, J.C. Smith[†]*, and T. Yoshida[†]*, Johnson Research Foundation, Univ. of Penna., Phila., PA 19174 and Bell Laboratories, Murray Hill, N.J. 07974

Oxonol, cyanine, merocyanine and naphthalene sulphonate dyes are widely used as indicators of membrane potentials. We have studied a homologous series of oxonol dyes which respond to changes of membrane potential in a wide variety of systems (1,2). Well-defined model membrane systems permit the analysis of many of the factors contributing to the overall spectral response. The dye-membrane interaction is characterized by spectral changes indicating the transfer of the dye to a hydrophobic environment. The kinetics of dye binding to lipid vesicles indicate that the probes are accessible to the interior and exterior membrane faces at very different rates and with a stoichiometry compatible with that derived from equilibrium measurements. The transmembrane distribution of the dyes is governed by factors related to their solubility in the phases separated by the membrane. Diffusion potentials across the vesicle membrane induced by specific ionophores generate spectral changes in the dyes additional to those of passive binding. Equilibrium measurements indicate contributions from altered dye binding and from changes in the bound dye. The magnitude of the response is non linear with potential which may indicate linear and quadratic electrochromic contributions to the overall response. Kinetic studies show that the rate at which the dyes respond to a diffusion potential is similar to the second order binding process and much faster than the first order dye-membrane dissociation. In oriented multilayers, the position of the transition moment of the dyes with respect to the plane of the membrane was established by polarized absorption spectroscopy. In such systems, application of an external field allows the direct study of electrochromism. 1) B.Chance and M.Baltscheffsky, *Biomembranes* 7:33(1975). 2) Smith, J.C. et al, *Biochem.*, in press. This work was supported by HL18708 and HL17826.

F-POS-N11 IRON-SULFUR CLUSTERS IN THE SUCCINATE DEHYDROGENASE. J. C. Salerno, Dept. of Biochemistry & Biophysics, University of Pennsylvania, Philadelphia, PA. 19174

Soluble succinate dehydrogenase (BS-SDH) contains 8 atoms of non-heme iron per flavin (1). The existence of two binuclear iron-sulfur clusters (S-1 and S-2) can be shown by quantitation of nonheme iron by the formation of paramagnetic complexes with NO; BS-SDH EPR spectra observed in 80 % DMSO show spectra characteristic of binuclear clusters (2). The HiPIP-type signal observable in the oxidized enzyme is characteristic of a tetranuclear iron-sulfur cluster (S-3) (3). The fully reduced enzyme shows evidence of spin coupling between Centers S-1 and S-2 in both the reconstitutively active (BS-SDH) and inactive (B-SDH) forms; broadening and splitting of the central $g=1.93$ resonance in BS-SDH and B-SDH, respectively, and desaturation of the S-1 EPR signals by paramagnetic S-2 in both cases are observed (1). The existence of spin coupling is demonstrated by the observation of half field signals characteristic of $\Delta m_s = 2$ transitions. Analysis of the power saturation of EPR signals from the fully reduced enzyme shows that Center S-2 has a shorter relaxation time in BS-SDH than in B-SDH, accounting at least in part for the difference in observed spectra. While the relaxation of Center S-1 in the succinate reduced enzyme can be accounted for by Orbach type processes ($J=90 \text{ cm}^{-1}$), the other binuclear iron-sulfur cluster (S-2) has rapid low temperature relaxation indicative of either anomalously low values of J or a different relaxation mechanism, possibly involving paramagnetic excited states of reduced S-3. The possible participation in electron transport of a metastable state identified with a low potential electron carrier such as S-2 in a fixed molecular environment will be discussed. Ref., (1) Ohnishi et al., (1976) *J. Biol. Chem.* 251, 2094. (2) Cammack (1975) *Biochem. Soc. Trans.* 3, 482. (3) Ohnishi et al., (1976) *J. Biol. Chem.* 251, 2105. (Supported by United States PHG GM 12202, GM 16767, HL 12576, and NSF BMS 7513459).

F-POS-N12 EFFECTS OF JAHN-TELLER INSTABILITY AND EXCITED STATE NUCLEAR DISTORTION ON RESONANCE RAMAN EXCITATION PROFILES OF COPPER TETRAPHENYLPORPHYRIN

J. A. Shelnutt^{*} and D. C. O'Shea, School of Physics, Georgia Institute of Technology, Atlanta, Georgia 30332

Resonance Raman spectra of copper tetraphenylporphyrin (CuTPP) in solution have been obtained throughout the visible and excitation profiles of selected lines have been constructed. The excitation profiles will be discussed in terms of a new theoretical approach¹ which includes the effects of electronic degeneracy of the resonant states. The "helping" mode behavior which has been discussed previously^{1,2} is dramatic in the excitation profile of the $392\text{cm}^{-1}(\text{p})$ line of CuTPP. Here, the maximum in the 392cm^{-1} line profile (due to other vibrational modes) is at $\approx 1400\text{cm}^{-1}$ above the 0-0 maximum with an intensity approximately 10 times that of the 0-0 Raman intensity. These degeneracy effects are essential to even a qualitative interpretation of the extensive excitation spectra of CuTPP as they must be for their biological counterparts. The results will also be compared to nickel etioporphyrin I and chromium tetraphenylporphyrin chloride excitation profiles which were recently reported.²

1. J. A. Shelnutt, L. D. Cheung, R.C.C. Chang, N-T. Yu, and R. H. Felton, submitted to *J. Chem. Phys.*
2. J. A. Shelnutt, N-T. Yu, R.C.C. Chang, L.D. Cheung, and R. H. Felton, in "Proceedings of the Fifth International Conference on Raman Spectroscopy," (eds., E. Schmid, J. Brandmuller, W. Kiefer, B. Schrader, H. Schrotter), Freiburg, 1976, p.336, H. F. Schulz Publ. Freiburg.

F-POS-01 EFFLUX OF DIVALENT CATIONS FROM PRE-LOADED MITOCHONDRIA, T.E. Gunter, J.S. Puskin K.K. Gunter, and P.R. Russell*

Chelation and isotope insertion techniques have been used to study efflux of Ca^{2+} and Mn^{2+} from previously loaded rat liver mitochondria. Several agents have been found which affect Ca^{2+} and Mn^{2+} effluxes differently. When an uncoupler, such as carbonyl cyanide *m*-chlorophenyl hydrazone (CCCP) is added to loaded mitochondria, rapid efflux of either Mn^{2+} or Ca^{2+} ensues. The divalent cation transport inhibitor ruthenium red, under these conditions, greatly retards Mn^{2+} , but not Ca^{2+} , efflux. Metabolic inhibitors, such as Antimycin A or cyanide, retard Mn^{2+} efflux in the presence of a chelating agent to a rate significantly less than that in the presence of the chelating agent alone. No effect of these inhibitors on Ca^{2+} efflux is observed. Addition of the proper amount of an uncoupler reduces Mn^{2+} efflux in the presence of a chelating agent to a rate even less than that observed with the chelating agent alone. These results strongly suggest that Mn^{2+} and Ca^{2+} efflux mechanism(s) may differ. It is possible that Mn^{2+} uses a Mg^{2+} efflux mechanism. At this time, it remains possible that these differences can be explained by different velocities of transport for Mn^{2+} and Ca^{2+} .

F-POS-02 THE POSSIBLE SITE OF SUPEROXIDE ANION AND HYDROGEN PEROXIDE GENERATION IN MAMMALIAN AND HIGHER PLANT MITOCHONDRIA. P.R. Rich*, W.D. Bonner, Jr. and A.L. Moore*, Dept. of Biochem. & Biophys., Johnson Res. Fndn., Univ. of Pennsylvania, Phila., PA 19174.

It has been known for some time that mammalian mitochondria possess an antimycin A-insensitive superoxide anion and hydrogen peroxide generating capacity. The site of superoxide production is thought to be at the level of ubiquinone. Similar results were obtained with higher plant mitochondria although a second route of antimycin A-insensitive hydrogen peroxide generation may occur, via the "alternative oxidase." It was found that salicylhydroxamic acid inhibited this alternative oxidase and also superoxide anion generation in both mammalian and higher plant mitochondria, although no effect upon the main respiratory pathways was detected. A further effect of salicylhydroxamic acid was noted upon the complex EPR signals split around $g=2.00$ which have been observed at temperatures close to that of liquid helium in both mammalian and higher plant mitochondria. The hydroxamic acid caused the splitting to disappear in all cases and the half maximal effect was observed at concentrations similar to those required for half maximal inhibition of superoxide anion production. This splitting has previously been ascribed to the interaction between two ubisemiquinone molecules, one of which is in close proximity to HiPIP center S-3 of succinate dehydrogenase. It is proposed from this data that the site of action of hydroxamic acids may be at the level of ubisemiquinone and that this species may be involved in superoxide anion generation in both mammalian and higher plant systems. Further, this process may not be dissimilar to the mechanism of the higher plant alternative oxidase.

F-POS-03 ENERGY-DEPENDENT EXTRUSION OF K^+ FROM HEART MITOCHONDRIA. E. Chávez* and G. P. Brierley, Dept. of Physiological Chem., Ohio State Univ., Columbus, Ohio 43210.

A slow, energy-dependent influx of $^{42}\text{K}^+$ can be demonstrated in isolated heart mitochondria in the absence of net uptake or loss of K^+ . The reaction shows saturation kinetics ($K_m=12 \text{ mM}$, $V=3 \text{ nmoles/min/mg}$), is inhibited competitively by Mg^{2+} ($K_i=3 \text{ mM}$), and, in agreement with Diwan et al. (BBRC 50, 384, 1973; J. Cell Biol. 67, 96a, 1975), is activated by P_i , thiol-group reagents, and by elevated pH. Under similar conditions, the efflux of K^+ from ^{42}K -labeled heart mitochondria is energy-dependent, occurs at low rates ($4-5 \text{ nmoles/min/mg}$), is inhibited by Mg^{2+} , and is strongly accelerated by P_i , mercurials, and by elevated pH. Optimal efflux with P_i and mercurials requires K^+ in the suspending medium ($K_m=30 \text{ mM}$). Na^+ replaces K^+ only in the presence of EDTA which increases Na^+ influx. Efflux of $^{42}\text{K}^+$ is not accelerated during massive energy-dependent uptake of K^+ and acetate in the absence of ionophores (in contrast to the result with P_i). Retention of ^{42}K under these conditions establishes that the mechanism for net uptake of K^+ differs from that responsible for steady-state $^{42}\text{K}^+$ exchange. Osmotic swelling and contraction studies have suggested that both a K^+ uniport (which depends on membrane potential, $\Delta\psi$, and is the pathway for net cation uptake) and a K^+/H^+ exchanger (which responds to transmembrane ΔpH and comes into play during net cation extrusion) are present in mitochondria (Brierley, Mol. Cell. Biochem. 10, 41, 1976). In the absence of regulatory mechanisms, the presence of both of these pathways would result in uncoupling and in high rates of turnover for mitochondrial K^+ . The present studies suggest that $^{42}\text{K}^+/\text{K}^+$ exchange results from a regulated interplay between K^+ uniport and K^+/H^+ exchange and is consequently activated by conditions which increase ΔpH , $\Delta\psi$, or K^+ permeability. They further implicate Mg^{2+} as a regulatory factor in the exchange. Supported by USPHS Grant HL-09364 and by the Central Ohio Heart Chapter.

F-POS-04 RESPIRATORY PROTON TRANSLOCATION AND MEMBRANE ENERGIZATION IN *E. COLI*. J. Michael Gould and W. A. Cramer, Dept. of Biol. Sciences, Purdue University, W. Lafayette, IN. 47907.

The addition of a small pulse of oxygen to an anaerobic suspension of log phase *E. coli* cells is known to induce a transient energization of the cell membrane which is accompanied by an efflux of protons into the external medium. In the absence of permeant ions to collapse the resulting membrane potential, the kinetics of H^+ efflux are slow (1st order, $t_{1/2} = 10s$) and the efficiency is low ($H^+/O \leq 0.5$). The slow kinetics for H^+ efflux and the low H^+/O ratio observed are independent of both the amount of oxygen added in the pulse and of the cell concentration, even to levels of O_2 /cell which are well below the levels required to maximally energize the membrane, indicating that the slow kinetics and low H^+/O values cannot be attributed to a respiratory control phenomenon. In an anaerobic cell suspension a small O_2 pulse causes a rapid decrease ($t_{1/2} < 0.5s$) in the fluorescence intensity of the probe N-phenyl-1-naphthylamine, followed by a slower relaxation of the fluorescence intensity to the original level. The extent of the rapid fluorescence decrease is proportional to the amount of O_2 added in the pulse, although the half-time for the subsequent fluorescence relaxation is independent of the amount of O_2 added. Colicin E1 and the uncoupler FCCP greatly increase the rate of relaxation of the fluorescence decrease, suggesting that the rapid fluorescence decrease is reporting the energization of the membrane, while the relaxation of the fluorescence decrease is reporting the subsequent deenergization of the membrane resulting from counterion redistributions. The fact that the efflux of H^+ into the medium after an O_2 pulse is small and much slower ($t_{1/2} = 10s$) than the energization of the membrane ($t_{1/2} < 0.5s$) suggests that the current of respiratory protons involved in the energization of the bacterial membrane may be occurring within rather than across the inner membrane.

Supported by NIH grant GM-18457 and NRSA #1F32GM9901301 (JMG).

F-POS-05 INTERACTIONS BETWEEN THE MITOCHONDRIAL AND MICROSOMAL ELECTRON CHAINS IN TOBACCO HORNWORM MIDGUT: EFFECTS ON ACTIVE TRANSEPITHELIAL K^+ TRANSPORT. L.J. Mandel, D.F. Moffett* and T.G. Riddle*, Dept. of Physiology and Pharmacology, Duke University Medical Center, Durham, N.C., 27710, and Dept. of Zoology, Washington State University, Pullman, Wash. 99163.

The midgut of the tobacco hornworm (*Manduca sexta*) actively transports K from hemolymph to lumen and the energy for this process appears to be intimately linked to oxidative metabolism. By mounting the excised tissue in a flattened version of an Ussing chamber with optical windows, we monitor concurrently the rate of active transport and the redox levels of the components of the respiratory chain under a variety of experimental conditions. It has been previously shown (Mandel, Moffett, and Jübsis, Biochim. Biophys. Acta 408:123, 1975) that the respiratory chain components are normal in this tissue, except for a large concentration of cytochrome b_5 . This latter cytochrome is predominantly localized in the microsomal fraction. The possibility of a direct interaction between electron transport in the mitochondrial chain and cytochrome b_5 was raised by Mandel, et al. (see above), because this cytochrome appears to act in redox synchrony with the mitochondrial chain components.

The present study provides additional evidence for the interaction between mitochondrial and microsomal electron chains. Sesamol and pyperonyl butoxide, known cytochrome P-450 inhibitors, cause: 1) an oxidation of cytochrome b_5 , 2) oxidation of the mitochondrial chain components, and 3) a profound inhibition of active transepithelial K transport. The effect of these inhibitors is probably through P-450, since they elicit a spectral peak at 440nm (characteristic of P-450) and they seem to have no effect on isolated mitochondria. The experimental evidence suggests that the interaction between these electron transport systems is involved in the energy conversion for active K transport.

F-POS-06 PROTON GRADIENT AND ENERGY COUPLING TO TRANSPORT OF CHLORTETRACYCLINE BY *Streptococcus faecalis*. E. V. Lindley* and J. A. Magnuson* Intr. by Richard Bockrath, Department of Microbiology, Indiana University School of Medicine, Indianapolis, Ind. 46202 and Program in Biochemistry and Biophysics, Washington State University, Pullman, Wash. 99163.

Accumulation of tetracycline antibiotics by *Streptococcus faecalis* occurs by active transport. Binding of the substrate was unchanged by the input of energy, while the maximal velocity increased significantly. Inhibition studies suggested that energy is coupled to the transport system by means of the protonmotive force. The degree of accumulation is dependent upon the energy state of the cells and the external substrate concentration. The pH gradient portion of the protonmotive force energized the accumulation system. An electrical potential formed by treating potassium-loaded cells with valinomycin did not activate transport, but an artificial proton gradient formed by treating proton-loaded cells with nigericin and potassium stimulated the accumulation of chlortetracycline. Proton extrusion in the apparent absence of ATP hydrolysis effectively activated the transport system.

F-POS-07 RELATIVE LOCATION OF THE CARDIAC GLYCOSIDE RECEPTOR AND DIVALENT CATION BINDING SITES IN THE Na-K ATPase STUDIED WITH FLUORESCENCE ENERGY TRANSFER. E.G. Moczydlowski*, and P.A.G. Fortes (Intr. by M. Montal), Biology Department, University of California, San Diego, La Jolla, California 92093

Ouabain binds to the external aspect of the Na-K ATPase (E), while Mg and ATP bind to the inside. Since we have a fluorescent analogue of ouabain, AO, that binds specifically to the cardiac glycoside receptor, we have studied the possibility of measuring the transmembrane distance of E with resonance energy transfer from AO to a suitable acceptor located on the inside. E activity and AO binding require Mg^{++} , but Mn^{++} and Co^{++} can substitute for Mg^{++} . Since the Co^{++} absorption spectrum overlaps the AO emission spectrum, Co^{++} should quench AO fluorescence arising from the cardiac glycoside receptor, if the sites are close enough and properly oriented. We found that Co^{++} bound to a high affinity site ($K_{0.14} \mu M$ for rabbit E and $\sim 20 \mu M$ for eel E) promotes AO binding without quenching AO fluorescence indicating that this site is either too far or not oriented to allow efficient energy transfer. A second type of Co^{++} site(s) has a lower affinity ($K_{0.4} mM$ for rabbit E and $\sim 0.7 mM$ for eel E) and is closer to the AO site since occupation by Co^{++} quenches AO fluorescence 85% (rabbit) and 50% (eel). Quenching is reversed by EDTA with no decrease in Co^{++} absorbance, ruling out filter effects. The low affinity Co^{++} site may be inhibitory since E activity decreases at Co^{++} concentrations that quench AO fluorescence. These results indicate that E has at least two functionally distinct divalent cation binding sites, located at different distances from the cardiac glycoside receptor. Knowledge of the relative orientations of AO and Co^{++} may allow accurate distance estimates between sites and quantitation of conformational changes induced by ligands. (Supported by a grant-in-aid from the American Heart Association and NIH grant RR-08135).

F-POS-08 SITE-DIRECTED FLUORESCENT PROBES OF THE Na-K ATPase. P.A.G. Fortes, A.J. Jesaitis* and E.G. Moczydlowski*, Biology Department, University of California, San Diego, La Jolla, California 92093

We have synthesized a fluorescent derivative of ouabain, anthroyl ouabain (AO), that binds specifically to the cardiac glycoside receptor of the Na-K ATPase (E). Specific AO binding requires Mg and results in increased quantum yield and characteristic spectral shifts which allow direct measurements of equilibria, kinetics and conformational transitions of the receptor. ATP, Pi, Na and K alter AO binding kinetics, allowing fluorimetric measurements of ligand binding constants. We have attempted to label other functional sites with probes that can act as energy transfer acceptors for AO. Trinitrophenyl ATP (TNP-ATP) is fluorescent (λ_{ex} : 410, 485 nm; λ_{em} : 540 nm) and binds to E with increased fluorescence and a blue shift. TNP-ATP binding is half-saturated at $0.4 \mu M$. ATP inhibits TNP-ATP binding, suggesting that it binds at an ATP site. Fluorescein mercuric acetate, (FMA, λ_{ex} : 495 nm, λ_{em} : 525 nm) inhibits E by reaction with SH groups which results in 85% decrease in quantum yield and a red shift. Bis-TNS ($10 \mu M$) and Bis-ANS ($20 \mu M$) inhibit E 100%, indicating that they bind to functional sites. These results suggest that information on the properties and location of active sites, labeled by these probes, the distances between them and the changes in conformation in different states may be obtained with fluorescence spectroscopy. (Supported by a grant-in-aid from the American Heart Association and NIH grants RR-08135 and GM-07169)

F-POS-09 A REPRODUCIBLE METHOD FOR OBTAINING HIGH YIELDS OF THE MITOCHONDRIAL SODIUM/POTASSIUM IONOPHORE. G.A. BLONDIN, INSTITUTE FOR ENZYME RESEARCH, UNIVERSITY OF WISCONSIN, MADISON, WI 53706.

The electrogenic Na^+/K^+ peptide ionophore (I) which we first isolated from beef heart mitochondria (BHM) in 1969 has been found to originate exclusively from a set of hydrophobic membrane proteins derived from BHM. A completely new method of isolation has been developed which circumvents the problems of poor yields and reproducibility which has marked this experimental program for over seven years. The key feature of the isolation derives from the finding that I can exist in two reversible forms; i.e., one which is electrogenic (I_e) and one which is non-electrogenic (I_{ne}). More importantly, the irreversible transformation of I_{ne} into I_e can be affected by treatment of the former with diazomethane. The yield of I_e (5 to 6 μgms per gm protein) and reproducibility of its isolation by present methods (over 50 consecutive successful isolations) has further enabled us to characterize I_e . The minimum M.W. of I_e from quantitative amino acid analysis of acid hydrolysates is 1580. The ionophorous activity of I_e in the presence of sodium or potassium ions is essentially the same as has been described for our earlier preparations of I. However, the heretofore unrecognized interaction of I_e in its present state of purity with calcium ions has been deduced from both equilibrium measurements and its ability to induce the active uptake of calcium ions in ruthenium red-inhibited BHM.

F-POS-010 MOLECULAR MECHANISM OF ACTION OF UNCOUPLER (U) ON MITOCHONDRIAL COUPLED PROCESSES. R.J. KESSLER*, C. TYSON*, H. VANDE ZANDE*, P. GLASSER*, AND D.E. GREEN, INSTITUTE FOR ENZYME RESEARCH, UNIVERSITY OF WISCONSIN, MADISON, WI 53706.

Uncoupling reduces to induction by classical uncouplers (U's) of cyclical transport of cations--a process excluding all other coupled processes. Three components are required--U, intrinsic electrogenic ionophore, and cation (mono- or divalent). In cyclical transport, U functions both as proton and cation carrier. In the latter capacity, U works synergistically with an intrinsic ionophore-cation complex. The supporting evidence includes: correlation of release of bound divalent cations by U's with emergence of uncoupler-insensitive respiration; essentiality of a critical level of bound or free cations for uncoupling; ionophoric and protonophoric capability of known U's; synergistic effect of U's and electrogenic ionophores (natural intrinsic ionophores or synthetic and antibiotic ionophores) in facilitating cation transport across a water-immiscible organic phase; 1:1 molar relation between U and electron during uncoupler-induced cyclical transport of cation driven by electron transfer. In cyclical transport of monovalent cations, electrogenic ionophore carries the cation into and across the membrane when coupled to the electron, whereas the ionophore-U complex carries cation passively across the membrane in the opposite direction. U's thus duplicate the action of uncoupling combinations (valinomycin + K^+ + nigericin) in inducing cyclical cation transport.

F-POS-011 FATTY ACIDS--PHYSIOLOGICAL UNCOUPLERS OF MITOCHONDRIAL COUPLED PROCESSES AND INDUCERS OF CYCLICAL CATION TRANSPORT. R.A. HAWORTH* (Intr. by H. KOMAI), INSTITUTE FOR ENZYME RESEARCH, UNIVERSITY OF WISCONSIN, MADISON, WI 53706

Mitochondria can fluctuate between two configurational states (Hunter et al., J. Biol. Chem., 251, 5069). Uncoupler-sensitive coupled ATP synthesis takes place in the aggregated configuration; uncoupler-insensitive cyclical transport of cations in the orthodox configuration. Evidence includes the 1:1 molar stoichiometry of H^+ ejection and K^+ uptake during a pulse experiment (injection of O_2); dependence of the rate of respiration on concentration of cations (monovalent or divalent) in the suspending medium; the absence of protonic or cationic gradients during steady state conditions. Fatty acids can potentiate the Ca^{2+} -induced aggregated to orthodox transition. When this transition is inhibited with EGTA, fatty acids can still duplicate some of the properties of the natural uncoupler responsible for cyclical transport in the orthodox configuration. Fatty acids, like uncouplers, are both cationic ionophores and protonophores forming 1:1 molar complexes with electrogenic ionophores and a cation (see abstract of R.J. Kessler et al.). The physiological uncouplers are latent in the phosphorylation mode and expressed in the cyclical cation transport mode of mitochondria. The insensitivity of mitochondria in the latter mode to added uncoupler reflects the presence and activity of intrinsic uncouplers.

F-POS-012 DETERMINATION OF PHOSPHORUS-31 DYNAMIC NMR PARAMETERS IN FROG MUSCLE AND MODEL SOLUTIONS. Sheila M. Cohen and C. T. Burt, University of Illinois at Chicago Circle, Chicago, Illinois 60680 and University of Illinois Medical Center, Chicago, Illinois 60612

Relaxation studies within living tissue have previously been limited to the study of either water or various ionic species such as ^{23}Na or ^{39}K . Phosphorus NMR however presents the possibility of measuring other metabolites. In particular, frog muscle has large quantities of phosphocreatine (PCr) which can be observed by ^{31}P NMR in reasonable time periods. Experiments at 3-5°C, where frog muscle is physiologically active, show little difference between spin-lattice relaxation time (T_1) for PCr in muscle and in the model solution. However, the spin-spin relaxation time (T_2) is depressed in muscle compared with these model solutions. Experiments must be done at this temperature to insure that changes in the amount of PCr with time are negligible. Time course studies of frog gastrocnemii show this criterion is satisfied for up to 5 hours under our conditions. Recently it has been appreciated that proton decoupled phosphorus can exhibit a nuclear Overhauser effect (NOE). The ^{31}P spectra of PCr solutions irradiated at the proton frequency show a pronounced NOE; in muscle we find the effect duplicates that of the model solution, both having a measured ($\eta+1$) of 2.00. Studies of the model solutions thus provide some insight into the dynamic interactions of PCr in intact muscle. (Work supported in part by Chicago Heart Assoc. and MDA.)

F-POS-013 CROSSLINKING OF BACTERIORHODOPSIN PROVIDES EVIDENCE OF DIFFERENT PROTEIN CONFORMATIONS IN THE DARK- AND LIGHT-ADAPTED STATE. T. Konishi and L. Packer, Membrane Bioenergetics Group, University of California, Berkeley, CA 94720.

Dimethylsuberimidate (DMS, 11.5 Å), dimethyladipimidate (DMA, 8.5 Å) and glutaraldehyde (GA, 7.5 Å) were used to treat bacteriorhodopsin (BR) in purple membrane preparations previously adapted to the light and dark state. 50-60% of lysine groups were modified by 10 mM DMA, 1 mM GA, or 20 mM ethylacetimidate (EA, 4.5 Å, the monofunctional control) treatment. Greater modification occurred in dark as compared to light-adapted BR, with DMA and GA. DMS did not show significant differences in extent of amidination between the two states. After treatment, BR was incorporated into lecithin liposomes. DMA- and GA-treated BR showed a marked difference in the retention of proton pump activity between light- and dark-adapted states, i.e. crosslinking of the dark-adapted BR inhibited proton pump activity more severely. EA and the longer chain DMS did not show significant differences in BR proton pump activity of dark- and light-treated samples. Spectra of crosslinked BR showed small changes in the region where aromatic amino groups absorb. Intrinsic fluorescence of tryptophanyl residues also decreased after crosslinking and appeared to coincide with loss of proton pump activity. GA treatment was made at the various stages in the dark after saturation illumination. Then, the rate of transition of the dark (560 nm λ_{max}) to the light-adapted state (570 nm λ_{max}), and the decay rate of the light- to dark-adapted state were measured from the 580-530 nm difference spectrum; these changes are partly inhibited after GA treatment. We conclude that two conformations of the BR protein exist in the dark- and light-adapted state; the latter conformation sustains greater proton pump activity. (Research supported by ERDA).

F-POS-014 PHOTOELECTRICAL POTENTIAL AND CURRENT GENERATIONS BY BACTERIORHODOPSIN ACROSS LIPID IMPREGNATED MILLIPORE FILTER MEMBRANES. P.K. Shieh and L. Packer, Membrane Bioenergetics Group, University of California, Berkeley, CA 94720.

Bacteriorhodopsin (BR) in the purple membrane of *Halobacterium halobium*, when excited by 570 nm light pumps protons and results in pH gradient across the membrane. When BR-liposomes interact with a polymer-stabilized black lipid membrane, photopotentials of about 200 mV are generated (BBRC 71:603, 1976). These studies on planar membranes plus BR-liposomes have been extended to the use of lipid-impregnated millipore filter membranes. Such filter membranes impregnated with soybean phospholipids and combined with BR-liposomes generate large photopotentials (220 mV) and photocurrents (1.8×10^{-8} amp/cm²). This photocurrent is about two orders of magnitude larger than usually can be observed in black lipid membranes. The magnitude of the photopotentials depends upon filter pore size (0.025-1.2 μ m), size of the BR proteoliposomes (200-2000 Å) and the nature of the lipids employed both for impregnating the filter and for making liposomes. Filter membranes are extremely stable, photopotentials with BR have been recorded during storage for five months. When BR-liposomes interact with the filter membrane, the photopotentials of about 220 mV can be enhanced in the presence of the proton ionophore *m*-chlorocarbonyl cyanide phenylhydrazine (4 μ M) photopotentials to 280 mV. The positively-charged cation triphenylmethylphosphonium ion (1 mM) which has been used to measure membrane potential gradients accompanying its partitioning across lipid membranes, collapses the photopotential. Hence lipid-impregnated filter membranes which are associated with BR-liposomes not only pump protons across the membranes but also are useful for monitoring the activity of substances which act as ionophores and membrane potential indicators. (Research supported by ERDA).

F-POS-015 SURFACE CHARGE OF THE INNER MITOCHONDRIAL MEMBRANE MONITORED BY IMPERMEABLE SPIN LABELS. A.T. Quintanilha and L. Packer, Membrane Bioenergetics Group, University of California, Berkeley, CA 94720.

Indirect methods are required to measure electrical forces developed across vesicular membranes. Partitioning of positively-charged cyanine dyes have been used to monitor charge separation but such probes are permeable and measure the transmembrane potential gradient across membranes (cf. Sims *et al.*, *Biochemistry* 13:3315, 1974). It is of interest to determine separately the charge at each membrane interface. A family of cationic spin labeled analogues of the detergent cetyl trimethyl ammonium bromide (CAT_n, n = 1-20) developed in this laboratory by Dr. R. Mehlhorn have been found to be useful as partitioning probes and to have long flip-flop rates in liposomes (cf. Abstracts, VII Internatl. Cong. Magnetic Resonance, St. Jovite, 19-24 Sept. 1976). Partitioning of CAT₁₂ in de-energized and energized mitochondrial inner membrane preparations was compared to that of an uncharged probe 2N11 and also to that of the positively-charged cyanine dye, 3,3'-dipropylthiodicarbocyanine iodide. When mitochondria are energized, the cyanine dye shows large changes in partitioning, even though CAT₁₂ or 2N11 do not. Partition changes can be obtained for the cyanine dye and CAT₁₂ by the addition of the unlabeled analogues of CAT_n. Thus, even though a large transmembrane potential is developed only a small change in surface charge occurs on the outer surface of the inner membrane. Upon de-energization both the dye and CAT₁₂ show large partitioning changes whereas 2N11 does not. It is concluded that impermeable charged spin label probes of the type used in the present study are useful indicators of membrane surface charge changes in closed vesicular systems. (Research supported by ERDA).

F-POS-016 HUMAN METABOLISM OF AFLATOXIN B₁: COMPARISONS AMONG INDIVIDUALS FOR PATTERNS OF HEPATIC DETOXIFICATION. D. M. Yourtee, D. L. Phillips*, and M. H. Flood*, Department of Biochemistry, Cancer Research Center, Columbia, Mo. 65201

While aflatoxin B₁ has shown mutagenic, teratogenic and carcinogenic properties in experimental test systems, the toxicology and biological fate of this mycotoxin in man requires substantial resolution. In the present study postmitochondrial fraction of human liver obtained at biopsy from a broad representation of donors has been employed in the *in vitro* metabolism of aflatoxin B₁. These investigations were conducted to obtain an estimation of the hazard of the food borne mycotoxin based on mass balances for toxicity classes of metabolites produced. In a population of sixteen specimens fourteen were active, transforming aflatoxin B₁ into several hydroxylated metabolites. These included in highest frequency aflatoxins M₁ and Q₁. Aflatoxin Q₁ presently recognized as among the least toxic of aflatoxins, has comprised commonly 50% or more of the modest turnover of initial aflatoxin B₁ radioactivity (¹⁴C) to organosoluble metabolites. Aflatoxin Q₁ has not been a product exclusively of either sex, age group, liver histology, or other subject parameters. However, trends have been evident suggesting suppressed formation of this metabolite, relative to other metabolites, for the older age group of the population from which the specimens were obtained. Overall results from *in vitro* work suggest by in large incomplete detoxification of aflatoxin B₁ by the human. In view of the possible formation of activated carcinogenic metabolites by human tissue implied in work of others the formation of metabolites such as aflatoxin Q₁ by humans *in vivo* can be recognized as critical in evaluating human risk. These considerations will be discussed further in relation to the most recent results for human tissue specimens.

F-POS-017 KINETIC MECHANISM OF THE GLUTAMATE-ASPARTATE TRANSLOCATOR. R. Viale*, K. Coll*, E. Murphy*, and J.R. Williamson Dept. Biochemistry and Biophysics, Univ. of Pennsylvania, Philadelphia, PA 19174

The kinetics of aspartate disappearance from mitochondria and appearance in the medium were followed after glutamate addition to aspartate loaded mitochondria at 10⁰. Intramitochondrial aspartate aminotransferase was inhibited by prior treatment of mitochondria with aminooxyacetate. Glutamate was varied from 1.5 to 15 mM, and pH from 6.4 to 7.8. Mitochondria were separated from the medium in sequential samples by rapid centrifugation through silicone oil. Data points of aspartate change with time were fitted by computer to the integrated Michaelis-Menten equation using the method of Fletcher and Powell. Apparent K_m and V_{max} values for internal aspartate and aspartate efflux were determined for each external glutamate concentration with a coefficient of variation less than 5%. The apparent K_m/V_{max} ratios and V_{max} values were found to be linearly related to glutamate concentration, thereby discounting a ping-pong mechanism. In order to define the kinetic mechanism more precisely aspartate efflux data points at five different glutamate concentrations were compared with curves generated using all the possible non-random, two substrate rate equations. An ordered bi-bi mechanism was indicated on the basis of the smallest least squares error term and non-negative kinetic constants. Values for concentration independent kinetic parameters at 10⁰ were: K_m external glutamate, 7.0 mM; K_m internal aspartate 3.7 mM; V_{max} = 23.1 nmoles/mg protein/min. The kinetic parameters measured in this manner were essentially independent of pH between 6.4 and 7.8. Using a Q₁₀ of 2.5 these kinetic constants have been used to calculate flux through the glutamate-aspartate translocator in the intact liver cell (see abstract this volume). Supported by NIH grants AM-15120 and HL-14461.

F-POS-018 CONTRIBUTION OF THE MALATE-ASPARTATE CYCLE TO REMOVAL OF CYTOSOLIC REDUCING EQUIVALENTS IN RAT LIVER CELLS. M.E. Tischler, P. Hecht*, R. Viale*, and J.R. Williamson. Dept. Biochemistry and Biophysics, Univ. of Pennsylvania, Philadelphia, PA 19174.

The major pathways for the transfer of reducing equivalents from cytosol to mitochondria in liver are the α-glycerophosphate and malate-aspartate cycles. Evaluation of each cycle's contribution has not been possible due to lack of a satisfactory inhibitor of the α-glycerophosphate cycle. Recent development of a technique for determining cytosolic and mitochondrial metabolite concentrations (Fed. Proc. 35, Abst#530, 1976) as well as elucidation of a rate equation for the mitochondrial glutamate-aspartate translocator (see abstract this meeting), has permitted us to calculate the contribution of the malate-aspartate cycle to overall transfer of reducing equivalents under different metabolic conditions. Flux through the glutamate-aspartate translocator was calculated from metabolic changes during incubation of liver cells. Flux a assumed 100% contribution of the malate-aspartate cycle, flux b assumed 100% contribution of the α-glycerophosphate cycle and flux c was calculated from measured mitochondrial and cytosolic aspartate and glutamate concentrations fitted to the translocator rate equation. With cells incubated with lactate, NH₃ and L-cycloserine (to inhibit the malate-aspartate cycle), aspartate efflux calculated as flux b and flux c agreed precisely. Thus % contribution of the malate-aspartate cycle can be calculated from the flux ratio (c-b)/(a-b). This value was found to vary under metabolic conditions associated with different intracellular concentrations of aspartate and glutamate. With lactate+NH₃ as substrates, the malate-aspartate cycle contributed 27%. After addition of ethanol or oleate flux through the malate-aspartate cycle was inhibited. The decrease was caused primarily by increased cytosolic aspartate, a noncompetitive inhibitor of the translocator. Supported by grants AM-15120 and GM-07229.

F-POS-P1 EFFECT OF INSULIN UPON THE MEMBRANE POTENTIAL OF FROG SARTORIUS MUSCLE. J.L. Rabovsky*, and R.D. Moore (Intr. by D. C. Lee) Section Biochem./Biophys. and Dept. Biology S.U.N.Y., Plattsburgh, N.Y. 12901.

The effect of insulin on the membrane potential of frog sartorius muscles incubated in 2.5 mM K⁺, 104 mM Na⁺ Ringer was examined. Insulin (250 mu/ml) hyperpolarized the membrane potential of freshly dissected muscles ($P < 0.025$) in each experiment by an average of 3.7 ± 1.2 (S.E.) mv. The hyperpolarization occurred by between 20 to 50 minutes after the addition of insulin. Fifty min. after addition of insulin, application of 10^{-4} M ouabain depolarized the membrane potential ($P < 0.005$ in each experiment) by an average of 5.4 ± 0.5 (S.E.) mv., to a level that was not significantly different ($P > 0.05$ in each experiment) from the level prior to the addition of insulin. The hyperpolarization observed on application of insulin to frog muscle agrees with the hyperpolarization observed when insulin was applied to rat muscle (Hazelwood & Zierler, 1967, Johns Hopkins Med. J. 121: 188). The insulin-induced increase in both net Na efflux (Moore, 1973, J. Physiol. 232:23) and in (Na⁺ + K⁺)-ATPase activity (Gavryck, Moore, & Thompson, J. Physiol. 252:43; 1975) is inhibited by cardioactive steroids. Accordingly, the inhibition by ouabain of the insulin-induced hyperpolarization observed in the present experiments suggests that insulin probably exerts its action upon the membrane potential by an action upon the Na pump.

F-POS-P2 EFFECT OF INSULIN UPON INTRACELLULAR pH. R. D. Moore, Section Biochem/Biophys, & Dept. Biology, S.U.N.Y., Plattsburgh, N.Y. 12901

A kinetic analysis of the effect of insulin upon active Na efflux from muscle (Moore, 1973, J. Physiol. 232:23) led to the prediction that insulin might increase intracellular pH, pH_i. The intracellular pH of frog (*Rana pipiens*) sartorius muscle was determined by the distribution of DMO-¹⁴C (¹⁴C 5,5-dimethyl-2,4-oxazolidinedione). Intracellular water was determined by subtracting extracellular water (as determined by sucrose-³H) from total muscle water. Intracellular DMO was estimated by effluxing DMO from the muscle for a two hour period and then using a computer program to back-extrapolate internal DMO to time zero in a manner which does not include the DMO in the extracellular space. In 15 normal untreated frog muscles (not exposed to insulin), the average intracellular pH determined in this manner was 7.13 ± 0.04 (S.E.). These muscles were the paired controls of muscles which were exposed to insulin (250 m.u./ml) for 90 minutes before estimation of intracellular pH. In 13 of the 15 experiments, the intracellular pH of the muscle exposed to insulin was greater than that of its paired control. The difference between the insulin-treated muscle and its paired control was $+0.134 \pm 0.03$ (S.E.) pH units and was statistically significant ($P < 0.005$). This suggests that insulin does indeed increase intracellular pH and it is likely that this is a mechanism whereby insulin regulates intracellular events such as glycolysis.

F-POS-P3 EXPERIMENTAL DETERMINATION OF THE TOTAL ARTERIAL COMPLIANCE AND THE TOTAL PERIPHERAL RUN-OFF AS A FUNCTION OF PRESSURE IN THE INTACT MAMMALIAN ARTERIAL SYSTEM. J. P. Dujardin* and H. P. Pieper, Department of Physiology, The Ohio State University, Columbus, Ohio 43210.

The interaction between the left ventricular pump and the arterial load can best be studied in the time domain. For this purpose an analog model of the arterial system has recently been developed and the components of this model have been measured *in vivo*. In order to determine the total arterial compliance and the total peripheral run-off as a function of pressure Wetterer and Pieper (1953) introduced the pressure-slope method. These authors assumed the diastolic pressure-decay to be a linear function of time. More accurate results are obtained when the diastolic decay is described by an exponential as measured *in vivo*. Using the result of this improved method, it is shown that the arterial system as seen from its input can be represented accurately by a four-component model. These four components were determined *in vivo* in six dogs.

This investigation was supported by a grant from the Central Ohio Heart Chapter of the American Heart Association and NIH grants HL-13900 and HL-18933.

F-POS-P4 TURBULENT FLOW PROPERTIES OF DILUTE SOLUTIONS OF RED BLOOD CELLS. H. Kutchai, J.B. Morton*, and M. Gad-el-Hak, Departments of Physiology and Engineering Science and Systems, University of Virginia, Charlottesville, Virginia 22901

The turbulent flow properties of dilute (0.06% by volume) suspensions of human red blood cells in 4 mm bore glass tubing were estimated by laser anemometry. The flow properties of the dilute red blood cell suspension were quite similar to those of a dilute suspension of polystyrene spheres (0.5 μ diameter) in isotonic NaCl solution. Flow was found to be laminar when the Reynolds number was below 2000, transitional in the range of Reynolds numbers between 2000 and 3000, and fully turbulent above Reynolds number 3000. The length and time scales of the turbulence were also estimated: at Reynolds number near 4000 the macroscale is about 1.25 mm, the Taylor microscale is near 0.85 mm and the Kolmogoroff scale is about 0.075 mm. These results are discussed in relation to previous measurements of the Reynolds numbers required to produce turbulent flow in more concentrated suspensions of red blood cells. Previous studies of the rate of oxygen uptake by dilute suspensions of red blood cells in the flow-type rapid reaction apparatus have employed similar experimental conditions to those we used. Our results suggest that under these conditions the turbulent flow of the red cell suspensions is characterized by eddies about 1 mm across which are mixing with each other on a time scale of about 45 msec (several time scales are required for complete mixing). Since most of the reported oxygen uptake measurements involve a similar time scale, it is possible that an effective "unstirred layer" influenced the reported rates of oxygen uptake.

F-POS-P5 TISSUE OXYGEN GRADIENTS: EVALUATION BY A 3-D STUDY OF REDOX TRANSITIONS IN ISCHEMIC AREA, ARTIFICIALLY PRODUCED IN THE PERFUSED RAT HEART. B. Quistorff, C. Barlow and B.Chance, Johnson Research Foundation, University of Pennsylvania, Philadelphia, PA 19174 USA.

Oxidized flavoprotein and reduced pyridine nucleotide are intrinsic probes of the mitochondrial redox state which can easily be measured by their specific fluorescence signals. Thus the ratio of the FP and PN fluorescence provides a sensitive measure of the mitochondrial redox state (1,2). These two parameters can be measured in frozen tissue with high resolution. Employing a recently developed scanning instrument it is possible to obtain a 3-D reconstruction of the redox structure of a frozen tissue where the single elements are smaller than 10^{-3} mm (3). The rat heart was perfused in a Langendorf perfusion with hemoglobin free medium and an ischemic area was produced by ligating a coronary artery giving rise to a localized ischemic area in the wall of the left ventricle. The size and position of the ischemic area was determined by NADH fluorescence photography (4). The heart was then freezeclamped with Wollenberger tongs and serial sections of the left ventricle wall scanned for the FP and PN signals in such a way that most of the ischemic area was well within the limitations of the scan. Displayed as FP/PN images all scans showed the ischemic area clearly demarcated by a sharp oxidation-reduction transition from perfused to nonperfused area. In some locations the transition was completed over a distance of less than 100 μ whereas it took 500 μ in others. Variation in the oxygen tension in the perfusate gave rise to a shift of the average width of the normoxia/anoxia transition zone, which allows estimation of the steepness of the oxygen gradient in the tissue.

1) B.Chance, et al, 10th FEBS Mtg., Paris, ABS 1657(1975). 2) B.Chance, *Circ.Res.* 35:I-69 (1976). 3) B.Quistorff and B.Chance, *Proc. APS Coll.*, Anaheim(1976). 4) C.Barlow and B.Chance, *Science* 193:909(1976). This work was supported by HL18708.

F-POS-P6 A CHEMIOSMOTIC MODEL FOR THE POLAR TRANSPORT OF AUXIN THROUGH PLANT TISSUE.

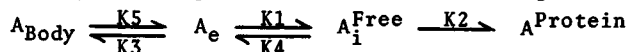
M.H.M. Goldsmith* and T.H. Goldsmith, Department of Biology, Yale University, New Haven, Conn. 06520.

Auxin (indoleacetic acid), a hormone regulating cell elongation in plants, is transported in shoots and roots i) polarly (i.e. to different extents in the two anatomical directions), ii) in the absence of an external concentration gradient, and iii) by a mechanism that requires energy metabolism. Recent evidence indicates that uptake of auxin by plant cells is regulated by a pH gradient maintained across the membranes by metabolism. Auxin, being a weak acid and lipophilic in the undissociated form, enters the cell primarily as HA. When the internal environment is at a higher pH than the external, however, a larger concentration of auxin anion (A^-) is in equilibrium with HA, and therefore auxin accumulates in the cell. The nature of the flux equilibrium will be altered if there is significant permeability to A^- .

Rubrey and Sheldrake and Raven have recently suggested that polar auxin transport might be dependent on a differential permeability to A^- at the apical and basal ends of the cells. We have formulated a computer model, applicable to transport in coleoptiles, and employing parameters (permeabilities, diffusion coefficient, membrane potentials, pH, cell dimensions) that can be either measured or reasonably estimated. The model assumes diffusion through the vacuoles and local flux equilibrium at each membrane. It successfully predicts appropriate distribution profiles vs time and section length, correct polar ratios, relative independence of through flux and net uptake, and inhibitory and stimulatory effects on transport when the cytoplasm is displaced by centrifugation.

F-POS-P7 TEMPERATURE EFFECTS ON THE UPTAKE OF L-LEUCINE BY TOADFISH LIVER IN VIVO. R. Persell* and A.E.V. Haschemeyer, Dept. of Biological Sciences, Hunter College, City University of New York, New York, New York 10021

A marine fish adaptable to a wide range of body temperatures has been used to examine the characteristics of L-leucine transport by liver at two temperatures in vivo. The experimental procedure involves injection of a bolus of fluid containing ^{14}C -L-leucine and ^3H -mannitol into the hepatic portal vein of the anesthetized fish. The recovery of the isotopes in the free and protein-bound fractions of liver and in blood leaving the liver is determined at times of 30s to 10 min after injection. The rate of disappearance of ^3H -mannitol from the liver provides a measure of blood flow and permits estimation of the amount of amino acid associated with extracellular space. Kinetic analysis was performed for the following model:



where the terms (left to right) represent fraction of amino acid in the body excluding the liver, in liver extracellular space, in liver intracellular free pool, and in liver protein. From the best-fitting values of the rate constants at 20° and 10°, the following temperature coefficients (Q_{10}) were obtained: 1.3 for k_3 and k_5 (blood flow); 3.8 for k_1 (influx); 2.8 for k_4 (efflux); 10 for k_2 (incorporation into protein). The results suggest a possible reduced contribution of active transport in leucine uptake at 10°.

F-POS-P8 THE ROLE OF PURINES, PYRIMIDINES AND NUCLEOSIDES ON COW RED CELL GLYCOLYSIS. M. J. Seider*, and Hyun Dju Kim, Dept. of Physiology, College of Medicine, University of Arizona, Tucson, AZ 85724.

Cow red cells, under normal physiological conditions, exhibit a comparatively low glycolytic rate of $0.56 \pm 0.05 \mu\text{moles/ml cell} \times \text{hr}$ with the lactate/glucose ratio of 1.52. This low glycolytic rate can be stimulated 70-80% above the basal rate by exogenously added adenosine. However, adenosine itself is sluggishly metabolized with the rate dependent upon substrate concentration. Moreover, inosine, which is impermeable to cow red cells, also stimulates glycolysis to a lesser extent. Of the purines and pyrimidine compounds thus far tested, xanthine, hypoxanthine, adenine and uracil have been found to stimulate cow red cell glycolysis. To ascertain the mechanism by which this stimulation of glycolysis takes place, three key glycolytic enzymes in hemolysates were examined in the presence of these stimulants. Adenine stimulated hexokinase activity from $.49 \pm 0.03 \mu\text{moles/gm Hb/min}$ to $.73 \pm 0.11 \mu\text{moles/gm Hb/min}$, whereas pyruvate kinase and phosphofructokinase were unaffected. Similarly inosine and hypoxanthine stimulated hexokinase activity. These data indicate that purines and nucleosides may exert their stimulatory effect on cow red cell glycolysis by increasing hexokinase activity.

Supported by NIH Grant AM-17723, and NIH Training Grant, HL-05884.

F-POS-P9 CATION TRANSPORT VARIANTS OF CHO CELLS WITH GREATER ABILITY TO PROLIFERATE IN LOW [K] MEDIUM. James S. Graves, Division of Biological Research, Ontario Cancer Institute, Toronto, Canada.

Reducing the [K] in the culture medium to levels below 1.0 mM slows the rate of proliferation of CHO cells, and prolonged exposure to 0.25 mM K medium causes appreciable cell death. From cultures exposed to 0.25 mM K medium for 4-6 d several clonal cell-lines have been isolated which are resistant to the cytotoxicity of low external [K]. In an attempt to determine the physiological alteration in one such variant, LK^{RA5}, I monitored the time-course of cell number, intracellular [Na] and [K], and the rate of protein synthesis during a 72 h exposure to 0.3 mM K medium in both A5 and the parental cell-type, WT. In these experiments A5 shows a moderate rate of proliferation after the first 24 h, while WT begins to proliferate slowly only after 48 h. In both cell-lines [K]_i decreases initially to about 40 mmol/l·cell and then recovers to the control level of >90 mmol/l·cell by 72 h. The early part of this recovery phase (i.e. 8-24 h) is slightly faster in A5 than in WT. The changes observed in [Na]_i differ markedly between WT and A5. In WT [Na]_i rises to greater than 100 mmol/l·cell by 24 h and is not reduced at 72 h. However, in A5 [Na]_i rises to about 90 mmol/l·cell at 24 h and is reduced to 50 mmol/l·cell by 72 h. The rate of protein synthesis (i.e. ^3H -leu incorp.) transiently decreases with [K]_i in both A5 and WT, and it appears unaffected by [Na]_i. The failure of WT cells to extrude Na while reaccumulating K could result from uncoupling of the Na-K pump under these conditions, and the lower [Na]_i maintained in A5 may be due to a more tightly coupled pump. Also, the data indicate that the long-term inhibition of proliferation by low [K] medium is not due to a permanent reduction in [K]_i or in protein synthesis, but high [Na]_i may be involved in this inhibition. Supported by a Medical Research Council of Canada grant to V. Ling and J.E. Till.

F-POS-P10 PROTEOLYTIC DISTINCTION OF L ANTIGENS ASSOCIATED WITH K^+ PUMP AND LEAK PATHWAYS IN LOW POTASSIUM SHEEP RED CELLS (LK SRBC). P.K. Lauf, B.J. Stiehl*, and C.H. Joiner*, Dept. of Physiology and Pharmacology, Duke University Medical Center, Durham, N.C. 27710.

Previous work from this laboratory (J. Memb. Biol. 4:52, 1971) established that anti-L serum failed to stimulate K^+ pump influx (^{86}Rb) in L antigen positive LK SRBC. We now report further studies on the mode and membrane specificity by which trypsin affects the response of the LK cation transport system to the L-antibody. Using newly prepared and unabsorbed L-antiserum which not only stimulated ^{86}Rb but also reduced ouabain insensitive K^+ leak influx (^{86}Rb) by 20-40%, we found that trypsin treatment of LK SRBC completely abolished the anti-L (anti- L_p) effect on ^{86}Rb but did not affect the antibody (anti- L_1) effect on ^{86}Rb . The effect of trypsin is highly specific for an attack on the L_p antigen associated with ^{86}Rb as demonstrated by a) a pronounced dependence on enzyme dose and incubation time, b) a failure of trypsin treated low and high potassium SRBC to inactivate the L antibody molecule, and c) by specific inhibition of proteolysis by equimolar amounts of the trypsin inhibitor ovomucoid. Furthermore, in trypsinized LK SRBC anti-L failed to stimulate the rate of 3H -ouabain binding above that found in control LK SRBC. Anti- L_p separated from anti- L_1 by adsorption to and elution from LK goat red cells failed to bind to trypsinized LK sheep RBC while anti- L_1 still reduced ^{86}Rb in untreated as well as trypsinized LK SRBC. These studies are conclusive proof that the L_p antigen associated with the LK pump is either destroyed or released from the LK SRBC membrane, while the L_1 antigen remains attached to the K^+ leak sites. Our findings are also consistent with our previous report (J. Memb. Biol. 28:351, 1976) that LK SRBC have more L antigenic sites than cation pumps. Initial attempts to find the L_p antigen in supernatants of trypsinized LK SRBC failed. (Supported by PHS HL 12 157)

F-POS-P11 INTERRELATIONS OF SERUM-SENSITIVE GROWTH STATE AND AMINO ACID UPTAKE IN A HUMAN FIBROBLAST: THE POSSIBLE ROLE OF THE MEMBRANE POTENTIAL. †Mitchel L. Villereal*, Emily Tate Brake*, and John S. Cook. Univ. Tenn.-Oak Ridge Graduate School of Biomedical Sciences, and Cancer and Toxicology Section, Biology Division, ORNL, Oak Ridge, TN 37830 USA.

The accumulation of α -aminoisobutyric acid (AIB) in subconfluent HSWP cells (a diploid human fibroblast) is sensitive to the concentration of serum in the growth medium. Cells growing in 10% fetal calf serum (normal cells) can accumulate AIB to concentrations ($AIB_{in}/AIB_{out} = 20-25$) which are 2-3 fold those attained in quiescent cells in 0.1% serum. Serum-stimulation of quiescent cells doubles their AIB concentrating capacity within 1 hr. AIB uptake in both normal and quiescent cells is dependent on the concentration of Na^+ in the medium. Accumulation of AIB is markedly sensitive to the K^+ diffusion gradient. As the K^+ gradient is dissipated by elevating external K^+ , the capacity for AIB accumulation in normal cells decreases to that seen in quiescent cells. The addition of valinomycin (Val) to cells pre-equilibrated with AIB causes an enhanced accumulation of AIB, suggesting that uptake may not be directly coupled to the K^+ gradient but rather may be influenced by changes in the membrane potential. The effect of Val on the accumulation of AIB is much greater in quiescent cells, with the intracellular AIB concentration reaching that seen in Val-stimulated normal cells. After pre-equilibration with AIB in 6 mM K^+ , transition to 94 mM K^+ + Val results in a marked and rapid net loss of AIB. In summary, these data suggest that the accumulation of AIB in HSWP cells may be influenced by growth-associated changes in membrane potential and that a membrane depolarization could be responsible for the decreased capacity for AIB accumulation in quiescent cells. [Supported by NCI and ERDA under contract with Union Carbide Corp. †Postdoctoral Investigator on Carcinogenesis Training Grant #CA 05296 from NCI.]

F-POS-P12 ΔpH AND TRANSMEMBRANE POTENTIAL IN ISOLATED CHROMAFFIN GRANULES. R. G. Johnson, N. Carlson,* and A. Scarpa, Dept. of Biochemistry and Biophysics, University of Pennsylvania, School of Medicine, Philadelphia, Pa. 19174.

It has recently been reported, based on [^{14}C]-methylamine distribution, that a ΔpH exists across the chromaffin granule membrane with the intragranular pH maintained at pH 5.50 irrespective of the pH of the surrounding medium (Johnson and Scarpa, J. Biol. Chem. 251 (1976), 2189). The methylamine distribution method was used to monitor the intragranular pH after addition of various concentrations of catecholamines. The addition of dopamine at concentrations greater than 1 mM (3-33 mM) collapses the ΔpH , the magnitude of the drop being from 1.25 pH units to 0.4 pH units in the presence of 33 mM dopamine. Ammonia produces a much more rapid collapse of the ΔpH than that induced by dopamine, while epinephrine and norepinephrine produce a much slower fall. Dopa, the dopamine precursor, has no effect upon the ΔpH . When the ΔpH collapse arises from catecholamine addition, the ΔpH can be re-established by the addition of ATP. Likewise, the simultaneous addition of ATP and dopamine prevents the ΔpH collapse. These effects of ATP are prevented in the presence of FCCP (carbonyl cyanide p-trifluoromethoxyphenylhydrazone), a proton translocator. When ATP is added to the granules in the absence of external catecholamines, a $\Delta \psi$ measured by [^{14}C] thiocyanate distribution is found to exist with a magnitude of 100 mV positive intragranularly. The further addition of FCCP causes the $\Delta \psi$ to reverse to a slightly negative value. These results suggest that catecholamine permeation may occur in the uncharged form and thus the distribution of catecholamines across the membrane may be dictated by the existence and magnitude of the ΔpH . The findings are also consistent with the existence of an inwardly directed proton pump which establishes the ΔpH and $\Delta \psi$ across the chromaffin granule membrane. (Supported by HL 18708 and GM 20246.)

F-POS-P13 EVIDENCE THAT $[ATP]^{3-}$ AND NOT $[ATPMg]^{2-}$ IS THE SPECIFIC SUBSTRATE OF THE ADENYLATE CYCLASE SYSTEM IN BARNACLE MUSCLE FIBERS. E.E. Bittar and R. Schultz*, Department of Physiology, University of Wisconsin, Madison, WI 53706.

Experiments with single muscle fibers from the barnacle, *Balanus nubilus* led to the suggestion that the stimulation of the Na efflux caused by adding protons to a HCO_3^- containing medium maybe due to activation of a cAMP-dependent protein kinase by newly formed cAMP. This idea has been tested by microinjecting .03M-protein inhibitor (isolated from rabbit muscle by D. Walsh) before or after reducing pH_e from 7.8 to 5.8. In both cases the protein inhibitor was found to completely abolish the stimulatory response (n=8). To decide which form of ATP is the specific substrate of the adenylate cyclase system (ACS), 0.5M-ATPMg and 0.5M-ATPNa₂ (at pH 7.0) were microinjected into fibers pretreated with 10^{-4} M-ouabain; the stimulation observed was in the order of $40.6 \pm 10.8\%$ (n=10) and $265.9 \pm 32.6\%$ (n=11), respectively. Injection of .01M-protein inhibitor following stimulation by injected .5M-ATPNa₂ resulted in partial reversal of the response ($35.6 \pm 5.1\%$, n=3). Injection of .5M-ATPNa₂ into poisoned fibers following reduction in pH_e from 7.8 to 6.3 resulted in $142.2 \pm 31.5\%$ (n=7) stimulation. The combined stimulatory response was reduced by $51.5 \pm 7.6\%$ (n=5) by injection of 0.01M-protein inhibitor. Parallel experiments done at pH_e 6.6 showed a $45.8 \pm 9.6\%$ reversal of the combined stimulatory response (n=3). And in experiments where restoration of pH_e from 6.6 to 7.8 was soon followed by injection of ATPNa₂, injection of protein inhibitor caused $38.8 \pm 6.1\%$ reversal (n=3). Taking into account that pH_i is about 6.6 when pH_e is 6.3 (^{14}C -DMO method) and that the pK for the reaction $-H^+ + [ATP]^{4-} \rightleftharpoons [ATP]^{3-}$ is 6.9, it would appear that $[ATP]^{3-}$ is the specific substrate for the ACS. (Supported by NSF and ONR).

F-POS-P14 ELECTROMECHANICAL COUPLING WITH SURFACE PHOSPHOLIPID CHARGES AND DIPOLES AS A MODEL FOR SALT RECEPTORS. J.A. DeSimone, J.D. Bond* and S. Price,* Department of Physiology, Medical College of Virginia, Richmond, Virginia 23298.

It has been suggested that charged phospholipids may constitute, at least in part, sites on taste cells for salt and acid reception. It is also possible that changes in taste cell membrane permeability may result from mechanical deformation of the receptor density resulting in characteristic changes in surface electrical potential. In order to gain insight into possible electromechanical coupling at a charged surface, we have investigated the effect of NaCl on the surface pressure of mixtures of dimyristoyl lecithin (DML) and dipalmitoyl phosphatidic acid (DPPA) at the heptane/solution interface. Increasing the salt concentration displaces the surface pressure (π) vs. area (A) isotherms to the right, i.e. for a given surface pressure, increasing the NaCl concentration results in decreased surface charge density. We obtain a theoretical expression for the isotherms based upon the Gibbs Adsorption Equation. The model assumes that the surface region consists of a narrow zone with low dielectric constant and a larger region beyond where the dielectric properties of the medium have their characteristic bulk values. The ions, including H^+ ions, distribute in the electrical double layer. At high ionic strength the double layer collapses and the H^+ ion concentration near the surface is low. By mass action the charged groups are highly ionized and the surface pressure is therefore high. At low ionic strength the surface H^+ ion concentration is high, and by mass action many of the charged groups are neutralized. The surface pressure is then lower. Our calculation explicitly includes both surface charge and dipole effects. The effects of surface charge alone are sufficient to give adequate qualitative agreement between theory and experiment.